Kinetics of Cloud Drop Formation and Its Parameterization for Cloud and Climate Models

Vitaly I. Khvorostyanov

Central Aerological Observatory, Dolgoprudny, Moscow Region, Russian Federation

Judith A. Curry

School of Earth and Atmospheric Sciences, Georgia Institute of Technology, Atlanta, Georgia

(Manuscript received XX Month 2007, in final form XX Month 2008)

Corresponding author address:

Dr. J. A. Curry
School of Earth and Atmospheric Sciences
Georgia Institute of Technology
Phone: (404) 894-3948
Fax: (404) 894-5638
curryja@eas.gatech.edu

Abstract

To study the kinetics of drop nucleation in clouds, the integro-differential equation for integral water supersaturation in cloud is derived and analyzed. Solving the supersaturation equation with an algebraic form of the cloud condensation nuclei (CCN) activity spectrum, analytical expressions are obtained for the time t_m of CCN activation process, the maximum supersaturation s_m, and droplet concentration $N_{dr}(s_m)$, limited by the total aerosol concentration at high supersaturations. All 3 quantities are expressed as functions of vertical velocity and characteristics of the CCN size spectra: mean geometric radius, dispersion, and parameters of solubility. A generalized power law for the drop activation, $N_{dr}(s_m) = C(s_m)s_m^{k(s_m)}$, is formulated that is similar in form to the Twomey's power law, but both the coefficient $C(s_m)$ and index $k(s_m)$ are functions of supersaturation expressed analytically in terms of vertical velocities and CCN microphysical parameters.

A simple and economical numerical solution was developed that describes all of these characteristics without conducting numerous simulations using parcel models. An extended series of numerical experiments was performed, in which the dependencies of t_m, s_m, $N_{dr}(s_m)$, $C(s_m)$, $k(s_m)$, and several other important characteristics of activation process were studied as functions of vertical velocity and physico-chemical properties of the aerosol. In particular, it is shown that a decrease in the condensation coefficient α_c leads to slower CCN activation, and higher maximum supersaturation and droplet concentration. Uncertainties in α_c may prevent correct estimates of the direct and indirect aerosol effects on climate. The solutions and expressions for the parameters presented here can be used for parameterization of the drop activation process in cloud and climate models.

1. Introduction

The concentration of cloud drops is an important parameter for both cloud and climate models. Precise evaluation of N_{dr} is required for simulation of the planetary albedo, cloud optical properties, and precipitation. In the initial stages of cloud formation, the number of cloud drops is directly related to the number of cloud condensation nuclei (CCN) that are activated. The CCN activity spectra are governed by the size and chemical composition of the aerosol particles and also the local supersaturation.

The CCN differential activity spectrum is written as:

$$\varphi_s(s) = dN_{dr}(s)/ds\,, \tag{1.1}$$

where N_{dr} is the number of cloud drops that are nucleated, and corresponds directly to the number of CCN that are activated at supersaturation s. The number of CCN actually activated is determined by the maximum supersaturation s_m reached in a cooling cloud parcel during CCN activation, which is determined by two competing processes: supersaturation generation due to adiabatic cooling and supersaturation absorption due to condensation growth of the newly formed drops. The final N_{dr} formed after the supersaturation has reached s_m is given by

$$N_{dr}(s) = \int_0^{s_m} \varphi_s(s')ds'\,. \tag{1.2}$$

which is referred to as the integral CCN activity spectrum (e.g., Pruppacher and Klett 1997, hereafter PK97). Thus, parameterization of N_{dr} according (1.2) requires knowledge of both $\varphi_s(s)$ and s_m.

Among the various methods for parameterizing the differential CCN spectrum $\varphi_s(s)$, we consider three different mathematical approaches: power law, lognormal and algebraic. The most commonly used power law approach was introduced by Twomey (1959)

$$\varphi_s(s) = C_T k s^{k-1}\,, \tag{1.3}$$

where the constant C_T and the index k are typically empirically determined. Substitution of (1.3) into (1.2) yields the corresponding power law

$$N_{dr}(s_m) = C_T s_m^k, \tag{1.4}$$

which has been widely used in cloud physics for almost five decades. The drawbacks of this parameterization are: the value of N_{dr} is not limited at high s_m and can exceed total CCN concentration N_a, and the parameters C_T and k are usually determined empirically from measurements of N_{dr} at varying values of s and are not related directly to the aerosol microphysical properties. Cloud chamber experiments have found a decrease of the index k with increasing s (e.g., Jiusto and Lala 1981; Ji and Shaw 1998; Yum and Hudson 2001; PK97), and hence there is no unique value of k. Subsequently, the index k has been related to the slopes ν of the aerosol size spectra by radius r in the form of inverse power laws as $f_a(r) \sim r^{-\nu}$ and aerosol soluble fraction (e.g., Buikov 1966; Levin and Sedunov 1966; Sedunov 1974; Jiusto and Lala 1981; Khvorostyanov and Curry 1999, hereafter KC99). This representation has shed some light on the nature of k and the power law (1.4), but if ν is constant independent of radius, this representation cannot explain the decrease of k with increasing s and does not solve the problem of unlimited increase of N_{dr} at high s.

Approximation of the aerosol size spectra by lognormal distributions leads to the same lognormal shape of $\varphi_s(s)$ and to parameterizations of $N_{dr}(s)$ expressed via the *erf* function that are limited at high values of s by the number concentration of aerosols N_a (e.g., von der Emde and Wacker 1993; Ghan et al. 1993, 1995; 1997; Abdul-Razzak et al. 1998; Abdul-Razzak and Ghan 2000; Nenes and Seinfeld 2003; Rissman et al. 2004; Fountoukis and Nenes 2005; Khvorostyanov and Curry 2006, 2007). The algebraic approach (Cohard et al. 1998, 2000) was based on a correction to Twomey's 2-parametric power law (1.3) by constructing $\varphi_s(s)$ in the form of an algebraic function with 4 empirical parameters. This introduced a correction to $N_{dr}(s)$

in the form of the Gauss hypergeometric function that ensured finite $N_{dr} \le N_a$ at high values of s, but added uncertainty in the choice of the 4 parameters.

The relationships among these three approaches were vague, and the degree of their agreement or disagreement was unclear. Each of these parameterization approaches is being used in cloud and climate models (with dominance of the power law). Khvorostyanov and Curry (2006, 2007, hereafter KC06, KC07) reconciled these three models by identifying the links and correspondence among their mathematical formulations and showed their equivalence. Further, a functional dependence of $\varphi_s(s)$ and $N_{dr}(s)$ was derived in KC06 as a generalized quasi-power law, similar to (1.3), (1.4) but with $C_T(s)$ and $k(s)$ as continuous analytical functions of s. These parameters were expressed directly via the aerosol physico-chemical parameters, and their decrease with s was such that it ensured the limit $N_{dr}(s) \le N_a$.

KC06, KC07 considered the activity spectra $\varphi_s(s)$, but treated supersaturation as a continuous variable, and hence the method developed in KC06, KC07 can be used as a refinement to the power law used in cloud models with prognostic supersaturation (e.g., in Morrison and Grabowski 2007), or in the analysis of chamber experiments, where the maximum supersaturation s_m can be calculated or measured and then $N_{dr}(s_m)$ determined (e.g. Yum and Hudson 2001; Kreidenweis et al. 2005; Svenningsson et al. 2006). Unfortunately, evaluation of supersaturation is a time-consuming procedure, and few cloud models such as short-term integrations of bin resolving models can afford the short time steps required to evaluate supersaturation explicitly as a prognostic variable. Bulk cloud and climate models do not have prognostic supersaturation equations, and thus have to use parameterizations for s_m and N_{dr} in terms of the predicted variables, most often expressing them as a function of the vertical velocity w similar to Twomey's (1959) original parameterization (e.g., Ghan et al. 1997; Lohmann et al. 1999; Saleeby and Cotton, 2004; Morrison et al., 2005a,b).

When s is not an independent continuous variable, but constrained by s_m due to interaction of the dynamical and microphysical factors, the applicability of the power law (1.4) becomes unclear. To ensure finite $N_{dr} \le N_a$ at high values of s, the indices k and coefficients C_T should be different at low and high values of s_m. However, it is uncertain in general, if s_m and the function $N_{dr}(s_m)$ can be described by the power law or quasi-power law with variable k and C_T. If so, analytical expressions are needed for s_m and N_{dr} that relate the values of k and C_T to aerosol microphysics and clouds dynamics.

Recent research has concentrated mostly on analytical parameterizations of the drop concentration, and their comparison with more precise parcel models. The use of the parcel models for tuning coefficients of parameterizations may bring in an additional uncertainty because of unavoidable differences among the models, e.g., in the radius size grids, time steps, various finite-difference approximations of supersaturation and drop growth equations, etc.

Further, variations in the basic assumptions (e.g., neglect of kinetic correction in the droplet growth rate, or variations in the condensation coefficient α_c) may require retuning the coefficients and rerunning the parcel models. Twomey (1959) and subsequent similar analytical parameterizations ignored the kinetic corrections. Abdul-Razzak et al. (1998), Abdul-Razzak and Ghan (2000) used a fixed value of the condensation coefficient α_c and noted that the use of any other value would require additional tuning with the parcel model. Fountoukis and Nenes (2005) accounted for the effects of α_c by averaging the effective vapor diffusion coefficient over some radius range, which requires additional determination of the limits of averaging, but did not present the explicit dependence $N_{dr}(\alpha_c)$.

Thus, a method for calculating drop activation kinetics is desirable that is not based on the parcel models, and allows changes in the basic assumptions like the kinetic correction to be accommodated more easily. For models with longer time steps that cannot accommodate a prognostic equation for supersaturation, a parameterization is needed that accounts for the time t_m

during which supersaturation reaches the value s_m and CCN activation proceeds, or the thickness of the activation layer. This requires analysis of the dependencies of t_m, s_m, N_{dr}, and other characteristics on the parameters of the CCN size spectra and chemical composition.

This paper extends the power law for drop activation by deriving relatively simple equations for t_m, s_m, N_{dr} in the form of the quasi-power laws that are functions of the vertical velocity and parameters of aerosol size spectra and chemical composition. In section 2, the basic assumptions on aerosol size spectra and activity spectra are briefly outlined. An equation for integral supersaturation is derived in section 3 and its solution is given in section 4 and compared with the previous solutions and parameterizations. Calculations of the kinetics of CCN activation and its major characteristics with variations of the input parameters over a wide range are described in section 5. Summary and conclusions are formulated in section 6.

2. CCN size and activity spectra

We assume that the size spectrum of dry aerosol $f_{ad}(r_{ad})$ by the dry radii r_{ad} can be approximated by the lognormal distribution with the aerosol number concentration N_a, the dispersion of the size spectrum σ_d, and the mean geometric radius r_{d0} related to the modal radius r_m as $r_m = r_{d0} \exp(-\ln^2\sigma_d)$. It was shown in KC06 that this lognormal spectrum is approximated with high accuracy by the algebraic spectrum

$$f_{ad}(r_{ad}) = \frac{k_{d0} N_a}{r_{d0}} \frac{(r_{ad}/r_{d0})^{k_{d0}-1}}{[1+(r_{ad}/r_{d0})^{k_{d0}}]^2}, \tag{2.1a}$$

where the index k_{d0} is as that introduced by Ghan et al. (1993)

$$k_{d0} = \frac{4}{\sqrt{2\pi}\ln\sigma_d}. \tag{2.1b}$$

This KC06 size spectrum behaves as the power law $f_{ad} \sim r_{ad}^{\,k_{d0}-1}$ at small $r_{ad} << r_{d0}$, and the Junge-type inverse power law $f_{ad} \sim r_{ad}^{\,-\nu}$ with $\nu = k_{d0} + 1$ at large $r_{ad} >> r_{d0}$. For typical

lognormal dispersions σ_d = 1.49, 1.7, and 2.2, the indices ν = 5, 4, and 3 respectively, which are the typical indices of the Junge spectra (Junge 1963; PK97). Similar values are obtained from the coagulation theory (PK97). This justifies the physical meaning of the algebraic spectrum (2.1a), which can be used as a generalization of the inverse power law, especially in the problems where the integrals of $f_{ad} \sim r_{ad}^{-\nu}$ diverge at small r as in aerosol optics. The size spectrum (2.1a) is related to the CCN activity spectrum using the Köhler equation for supersaturation $s = (\rho_v - \rho_{vs})/\rho_{vs}$ that can be written for dilute solutions as (PK97, Curry and Webster 1999):

$$s = \frac{A_k}{r} - \frac{B}{r^3}. \tag{2.2}$$

$$A_k = \frac{2M_w\varsigma_{sa}}{RT\rho_w}, \qquad B = \frac{3\nu\Phi_s m_s M_w}{4\pi M_s \rho_w}. \tag{2.3}$$

Here ρ_v, ρ_{vs} and ρ_w are the densities of vapor, saturated vapor and water, A_k is the Kelvin curvature parameter, M_w is the molecular weight of water, ζ_{sa} is the surface tension at the solution-air interface, R is the universal gas constant, T is the temperature. The parameter B describes effects of the soluble fraction, ν is the number of ions in solution, Φ_s is the osmotic potential, m_s and M_s are the mass and molecular weight of the soluble fraction.

It is convenient to parameterize the soluble fraction of CCN and parameter B following Levin and Sedunov (1966), KC99, KC06, KC07 as

$$B = br_{ad}^{2(1+\beta)}, \tag{2.4}$$

where the parameters b and β depend on the chemical composition and physical properties of the soluble part of an aerosol particle. The value β = 1/2 corresponds to the soluble fraction of an aerosol particle proportional to its volume (as for internally mixed aerosol) and the value β = 0 corresponds to the soluble fraction proportional to the surface (e.g., for a dust particle covered by a soluble film; Levin et al. 1996; Wurzler et al. 2000; Bauer and Koch 2005).

The parameter b can be expressed via the quantities defined in (2.3). For $\beta = 0.5$, b is a dimensionless parameter:

$$b = (\nu\Phi_s)\varepsilon_v \frac{\rho_s}{\rho_w}\frac{M_w}{M_s}. \tag{2.5}$$

where ρ_s is the density of the soluble fraction, ε_v is its volume fraction. For $\beta = 0$, the particle volume fraction was parameterized in KC99, KC06, KC07 as $\varepsilon_v(r_{ad}) = \varepsilon_{v0}(r_{ad1}/r_{ad})$, where r_{ad1} is some scaling parameter and ε_{v0} is the reference soluble fraction (dimensionless).

$$b = r_{ad1}\varepsilon_{v0}(\nu\Phi_s)\frac{\rho_s}{\rho_w}\frac{M_w}{M_s}. \tag{2.6}$$

For this case, b has the dimension of length and is proportional to the scaling radius r_{ad1}.

The size spectrum (2.1a) corresponds to the lognormal differential activity spectrum (e.g., Abdul-Razzak et al. 1998; Fountoukis and Nenes 2005; KC06, KC07). In KC06, KC07, this was formulated as

$$\varphi_s(s) = \frac{N_a}{\sqrt{2\pi}(\ln\sigma_s)s}\exp\left[-\frac{\ln^2(s/s_0)}{2\ln^2\sigma_s}\right], \tag{2.7}$$

where we introduced the mean geometric supersaturation s_0 and the supersaturation dispersion σ_s:

$$s_0 = r_{d0}^{-(1+\beta)}\left(\frac{4A_k^3}{27b}\right)^{1/2}, \tag{2.8}$$

$$\sigma_s = \sigma_d^{(1+\beta)}. \tag{2.9}$$

The modal supersaturation s_m is related to s_0 analogously to the dry size spectrum,

$s_m = s_0\exp(-\ln^2\sigma_s)$.

It was found in KC06, KC07 that the lognormal size spectrum and activity spectrum (2.7) or algebraic size spectrum (2.1a) correspond to the algebraic differential activity spectrum

$$\varphi_s(s) = \frac{k_{s0}N_a}{s_0}\frac{(s/s_0)^{k_{s0}-1}}{[1+(s/s_0)^{k_{s0}}]^2} \tag{2.10}$$

$$= k_{s0} C_0 s^{k_{s0}-1} (1+\eta_0 s^{k_{s0}})^{-2}, \tag{2.11}$$

where the index k_{s0} is an analog in s-space of k_{d0} defined in (2.1b) for r_d - space

$$k_{s0} = \frac{4}{\sqrt{2\pi}\ln\sigma_s} = \frac{4}{\sqrt{2\pi}(1+\beta)\ln\sigma_d}, \tag{2.12}$$

$$C_0 = N_a s_0^{-k_{s0}} = N_a \left(\frac{27b}{4A_k^2}\right)^{k_{s0}/2} (r_{d0})^{k_{s0}(1+\beta)}, \tag{2.13}$$

$$\eta_0 = s_0{}^{-k_{s0}} = \left(\frac{27b}{4A_k^2}\right)^{k_{s0}/2} (r_{d0})^{k_{s0}(1+\beta)}. \tag{2.14}$$

The first term before the parenthesis in (2.11) resembles Twomey's power law (1.3); however, the parameters (C_0, k_{s0}) in (2.11) are not empirical but are expressed via the aerosol physico-chemical properties. The second term in parenthesis in (2.11) decreases at large $s >> s_0$ as $s^{-2k_{s0}}$, ensuring the asymptotic decrease $\varphi_s(s) \sim s^{-k_{s0}-1}$ and serving effectively as a correction to the Twomey law since it prevents an unlimited growth of $N_{dr}(s)$ at large supersaturation.

Droplet or CCN concentration in algebraic form was derived in KC06, KC07 by integration of the algebraic CCN spectrum $\varphi_s(s)$ (2.10) or (2.11) over s:

$$N_{dr}(s) = N_{CCN}(s) = \int_0^s \varphi_s(s')ds'$$

$$= N_a \frac{(s/s_0)^{k_{s0}}}{[1+(s/s_0)^{k_{s0}}]} = C_0 s^{k_{s0}} [1+\eta_0 s^{k_{s0}}]^{-1}, \tag{2.15}$$

where C_0, k_{s0}, and η_0 are defined in (2.12) - (2.14). Again, the first term resembles Twomey's power law for the integral activity spectrum (1.4), and the second term in parentheses is a correction that ensures finite $N_{dr}(s)$ at high s. It was shown in KC06 that these expressions can be written as a generalized quasi-power law

$$N_{dr}(s) = C(s) s^{k(s)}, \tag{2.16}$$

where the coefficient $C(s)$ and index $k(s)$ are the functions of supersaturation

$$C(s) = N_a(s)s^{-k(s)} = C_0 s^{\chi(s)}[1+(s/s_0)^{k_{s0}}]^{-1}, \quad (2.17)$$

$$k(s) = k_{s0}[1+(s/s_0)^{k_{s0}}]^{-1}, \quad (2.18)$$

$$\chi(s) = k_{s0}(s/s_0)^{k_{s0}}[1+(s/s_0)^{k_{s0}}]^{-1}. \quad (2.19)$$

These equations are used in the next sections to derive expressions for t_m, s_m, and N_{dr} as functions of vertical velocity and the aerosol microphysical parameters.

3. Equations for supersaturation

When an air parcel rises adiabatically, the relative humidity increases as the parcel cools, reaching saturation at some level, and then CCN activation begins as the parcel becomes slightly supersaturated. The parcel supersaturation is governed by two competing processes: supersaturation generation by the rising motion and supersaturation absorption by the drops in the condensation process. This process can be described by the supersaturation equation, which we use in the form from Khvorostyanov and Curry (2005):

$$\frac{1}{(1+s)}\frac{ds}{dt} = c_1 w - \frac{\Gamma_1}{\rho_v} I_{con}, \quad (3.1)$$

where

$$c_1(T) = \left(\frac{L_e}{c_p T}\frac{M_w}{M_a} - 1\right)\frac{g}{R_a T}, \quad (3.2)$$

L_e is the specific latent heat of evaporation, c_p is the specific heat capacity of air, T is the temperature, R_a is the specific gas constant for air, M_w and M_a are the molecular weights for water and dry air, and Γ_1 is the psychrometric correction associated with the latent heat release at condensation

$$\Gamma_1 = 1 + \frac{L_e^2}{c_p R_v T^2}\frac{\rho_{ws}}{\rho_a}. \quad (3.3)$$

The vapor flux I_{con} to the droplets is the integral of the mass growth rate over the size spectrum that is expressed via growth rate $\dot{r}_d$ of the droplet radius r_d

$$I_{con} = 4\pi\rho_w \int_0^\infty r_d^2 \dot{r}_d f(r_d, t) dr_d \ , \tag{3.4}$$

where $f_d(r_d)$ is the size distribution function of the newly formed drops. We use $\dot{r}_d$ in the form

$$\dot{r}_d = \frac{c_3 s}{r_d + \xi}, \qquad c_3 = \frac{D_v \rho_{vs}}{\rho_w \Gamma_1}, \tag{3.5a}$$

$$\xi = \frac{4D_v}{\alpha_c V_w}, \qquad V_w = \left(\frac{8RT}{\pi M_w} \right)^{1/2} \tag{3.5b}$$

where D_v is the water vapor diffusion coefficient, ξ is the kinetic correction to the radius growth rate, V_w is the thermal speed of water vapor molecules, R is the universal gas constant, and α_c is the condensation coefficient. This equation for dr/dt (e.g., Fuchs 1959; Sedunov 1974) is equivalent to that given in PK97 (chapter 13), and accounts for the kinetic correction ξ.

Substitution of (3.5a) into (3.4) yields

$$I_{con}(t) = s(t) \frac{4\pi D_v \rho_{vs}}{\Gamma_1} \int_0^\infty \frac{r_d^2(t, t_0)}{r_d(t, t_0) + \xi} f_d(r_d, t) dr_d \ . \tag{3.6}$$

Here $r_d(t,t_0)$ denotes the radius at time t of a drop activated at time t_0. The radius $r_d(t,t_0)$ is evaluated from (3.5a)

$$r_d(t, t_0) = \{ [r_d(t_0) + \xi]^2 + 2c_3 [y(t) - y(t_0)] \}^{1/2} - \xi \ , \tag{3.7}$$

where $r_d(t_0)$ is the initial drop radius at the activation time, and $y(t)$ is the integral supersaturation

$$y(t) = \int_0^t s(t') dt' \ . \tag{3.8}$$

To express the size spectrum $f(r_d)$ via the activity spectrum, we apply a kinetic equation

$$\frac{\partial f_d(r_d)}{\partial t} + \frac{\partial}{\partial r} (\dot{r} f_d) = \varphi_s(s) \delta(r - r_d(t_0)) \ , \tag{3.9}$$

where $\varphi_s(s)$ is the differential activity spectrum, and δ is the Dirac delta-function. A solution to this equation describes the conservation law for the concentration of the newly formed drops and CCN

$$f_d(r_d) = \varphi_s(s)\frac{ds}{dt_0}\frac{dt_0}{dr_d}. \tag{3.10}$$

Substituting (3.7) - (3.10) into (3.6) yields

$$I_{con}(t) = s(t)\frac{4\pi D_v \rho_{vs}}{\Gamma_1}\int_0^t r_{ef}(t,t_0)\varphi_s(s)\frac{ds(t_0)}{dt_0}dt_0, \tag{3.11a}$$

where the integration is performed over the initial times of activation t_0 and

$$r_{ef}(t,t_0) = \frac{\{[(r_d(t_0)+\xi)^2 + 2c_3(y(t)-y(t_0))]^{1/2} - \xi\}^2}{[(r_d(t_0)+\xi)^2 + 2c_3(y(t)-y(t_0))]^{1/2}}. \tag{3.11b}$$

As shown below, variations of α_c (or ξ) can have substantial effects on activation process, especially for small α_c. The method developed provides solutions for any value of α_c as described in sections 4, 5, and allows examination of variable α_c and the kinetic correction ξ without running parcel models, and more generally than it was done in some previous works as discussed in Introduction.

Substituting $\varphi_s(s)$ from (2.11) into (3.11a) and using the relations $s = y'$, $\rho_v \approx \rho_{vs}$, yields the 2nd (relaxation) term on the right hand side in (3.1) in the form

$$\frac{\Gamma_1}{\rho_v} I_{con}(t) = y'(t)[4\pi D_v N_a J_0(t)] = \frac{y'(t)}{\tau_{p,ac}(t)}. \tag{3.12}$$

where $\tau_{p,ac}$ is the effective supersaturation relaxation time during this stage of drop formation,

$$\tau_{p,ac}(t) = [4\pi D_v N_a r_{act}(t)]^{-1}, \tag{3.13}$$

where $r_{act}(t) = J_0(t)$ is some activation radius, and the integral $J_0(t)$ has the dimension of length

$$J_0(t) \equiv r_{act}(t) = \frac{k_{s0}}{s_0^{k_{s0}}}\int_0^t r_{ef}(t,t_0)\frac{[y'(t_0)]^{k_{s0}-1}\, y''(t_0)}{\{1+\eta_0[y'(t_0)]^{k_{s0}}\}^{\mu}}dt_0. \tag{3.14}$$

The primes hereafter denote time derivatives. Note that with the KC06 activity spectrum (2.11), we have in the denominator of integrand $\mu = 2$, but we will retain the general notation μ for easier comparison with another models.

Now, using (3.12) - (3.14), the supersaturation equation (3.1) becomes

$$[1 + y'(t)]^{-1} y''(t) = c_1 w - y'(t)[\tau_{p,ac}(t)]^{-1}$$

$$= c_1 w - y'(t)[4\pi D_v N_a J_0(t)]\,. \tag{3.15}$$

This is a nonlinear integro-differential equation for the integral supersaturation $y(t)$ that governs the kinetics of the drop formation. Numerous previous attempts have shown that analytical solution is not feasible without simplifications. These simplifications and solutions are considered in the next section.

4. Solutions to the supersaturation equation

Solutions to the supersaturation equation (3.15) should yield the maximum value s_m of supersaturation in a rising parcel, the time t_m when s_m is reached, and the concentration N_{dr} of the activated drops. This solution requires evaluation of the integral J_0 in (3.14). It is convenient to introduce a new integral J_1 and rewrite (3.15) as

$$[1 + y'(t)]^{-1} y''(t) = c_1 w - c_4 y'(t) J_1(t)\,. \tag{4.1}$$

Here

$$J_1(t) = \frac{s_0^{k_{s0}}}{(2c_3)^{1/2} k_{s0}} J_0(t)$$

$$= \int_0^t \frac{r_{ef}(t,t_0)}{(2c_3)^{1/2}} \frac{[y'(t_0)]^{k_{s0}-1} y''(t_0)}{\{1+\eta_0[y'(t_0)]^{k_{s0}}\}^{\mu}} dt_0\,, \tag{4.2}$$

with $r_{ef}(t,t_0)$ defined in (3.11b), and

$$c_4 = 4\pi D_v N_a (2c_3)^{1/2} k_{s0} s_0^{-k_{s0}}\,, \tag{4.3}$$

c_3 is defined in (3.5a) and we retain the general index μ in the denominator.

Note that (4.1) differs from the usually used supersaturation equations (e.g., PK97, Seinfeld and Pandis 1998, and most works cited here): a) it deals with the integral and not with the differential supersaturation; b) it is of 2nd order with respect to the integral supersaturation y but operates only with y and its derivatives; c) the last term, which describes the sink of vapor onto the droplets, is expressed via y' (i.e., directly supersaturation) in contrast to typically used derivative $d(LWC)/dt$ with implicit dependence on s. This form of the equation is convenient both for analytical solutions and numerical models of various complexity.

The form of (4.1) suggests that the first iteration to the solution can be sought substituting the first term on the right-hand side into the 2nd term, i.e.,

$$y'' = c_1 w, \qquad y'(t) = s(t) = c_1 w t, \qquad y(t) = (c_1 w/2)t^2. \tag{4.4}$$

This method with a linear approximation for $s(t)$, first developed by Twomey (1959) and used later by many authors (e.g., Sedunov 1967, 1974; Ghan et al. 1993; Abdul-Razzak et al. 1998), gives an upper limit for $J_1(t)$, and lower limit for $s(t)$, and approximates a solution to good accuracy. Substituting (4.4) into (4.2) yields

$$J_1 = \frac{1}{\sqrt{2}}(c_1 w)^{k_{s0}+1/2} t^{k_{s0}+1} J_2, \tag{4.5}$$

where J_2 is a dimensionless integral

$$J_2 = \int_0^1 \frac{\{[U_s + (1-x^2)]^{1/2} - V_s\}^2}{[U_s + (1-x^2)]^{1/2}} \frac{x^{k_{s0}-1}}{(1+\chi_s x^{k_{s0}})^{\mu}} dx, \tag{4.6}$$

and the three dimensionless variables are

$$\chi_s = \eta_0 (c_1 w t)^{k_{s0}} = \left(\frac{c_1 w t}{s_0}\right)^{k_{s0}}, \tag{4.7a}$$

$$U_s = \frac{[r_d(t_0) + \xi]^2}{c_3 (c_1 w) t^2}, \qquad V_s = \frac{\xi}{[c_3 (c_1 w)]^{1/2} t}. \tag{4.7b}$$

Substitution of $x^2 = z$ in J_2 yields

$$J_2 = \frac{1}{2} J_3, \qquad J_3 = \int_0^1 \frac{\{[U_s + (1-z)]^{1/2} - V_s\}^2}{[U_s + (1-z)]^{1/2}} \frac{z^{k_{s0}/2-1}}{(1+\chi_s z^{k_{s0}/2})^{\mu}} dz \,. \tag{4.8}$$

The integral J_3 can be evaluated analytically in some approximations or numerically as discussed below. Eq. (4.1) can be rewritten now as

$$[1+y'(t)]^{-1} y''(t) = c_1 w - \left(\frac{c_4}{2\sqrt{2}} \right) (c_1 w)^{k_{s0}+3/2} t^{k_{s0}+2} J_3(t) \,. \tag{4.9}$$

The time t_m when supersaturation in the parcel reaches a maximum s_m is determined from the condition $s'(t_m) = 0$, or $y''(t_m) = 0$, then the left hand side of (4.9) is zero and we obtain an algebraic expression for t_m,

$$t_m^{k_{s0}+2} = \frac{2\sqrt{2}}{c_4 J_3(t_m)} (c_1 w)^{-(k_{s0}+1/2)}$$

$$= c_5^{-1} N_a^{-1} s_0^{k_{s0}} (c_1 w)^{-(k_{s0}+1/2)} [J_3(t_m)]^{-1}, \tag{4.10}$$

where

$$c_5 = 2\pi D_v c_3^{1/2} k_{s0} \,. \tag{4.11}$$

Solving for t_m, after some transformations we obtain

$$t_m = K_{tms} N_a^{\frac{-1}{(k_{s0}+2)}} s_0^{\frac{k_{s0}}{(k_{s0}+2)}} w^{\frac{-(k_{s0}+1/2)}{(k_{s0}+2)}}, \tag{4.12}$$

$$K_{tms} = [c_1^{(k_{s0}+1/2)} c_5 J_3(t_m)]^{\frac{-1}{(k_{s0}+2)}} \,. \tag{4.13}$$

The maximum supersaturation can now be evaluated using (4.4) as $s_m = c_1 t_m w$, which yields

$$s_m = K_{sms} N_a^{\frac{-1}{(k_{s0}+2)}} s_0^{\frac{k_{s0}}{(k_{s0}+2)}} w^{\frac{3}{2(k_{s0}+2)}} \tag{4.14}$$

$$K_{sms} = [c_1^{-3/2} c_5 J_3(t_m)]^{\frac{-1}{(k_{s0}+2)}} \tag{4.15}$$

Finally, the drop concentration can be calculated from (2.15) or (2.16) with $s = s_m$

$$N_{dr}(s_m) = N_a \frac{(s_m / s_0)^{k_{s0}}}{1 + (s_m / s_0)^{k_{s0}}} = C_0 s_m^{k_{s0}} [1 + \eta_0 s_m^{k_{s0}}]^{-1} \tag{4.16}$$

$$= C(s_m) s_m^{k(s_m)}, \tag{4.17}$$

and $C(s_m)$, $k(s_m)$ defined in (2.17), (2.18). Eq. (4.17) represents the generalized power law with coefficient C and index k that are each functions of the maximum supersaturation or of the vertical velocity.

Eqs. (4.14) - (4.17) for s_m, $N_{dr}(s_m)$ represent a generalization of the corresponding expressions (1.4) from Twomey (1959) that were based on the power law (1.3), and convert into them if $\chi_s = 0$ or $\mu = 0$ (power law (1.3) for $\varphi_s(s)$ instead of algebraic KC06 spectrum (2.11) with $\mu = 2$), or $U_s = 0$, and $V_s = 0$ (initial radius $r_d(t_0) = 0$, and kinetic correction $\xi = 0$). When $\mu = 2$ and the other parameters are nonzero, these equations contain the integral J_3, which itself depends on t_m described by the new Eqs. (4.12), (4.13). However, (4.12) - (4.17) are easy for computing and for the compilation of lookup tables. Then $N_{dr}(s_m)$ can be calculated in a cloud or climate model using the modified power law (4.17) and these lookup tables, or using the asymptotic limits of the power law. All calculations below are made with the algebraic $\varphi_s(s)$ (2.11), i.e., $\mu = 2$.

The primary equation is (4.12), since once we know t_m, we can calculate s_m and $N_{dr}(s_m)$. The method of calculating t_m is illustrated in Fig. 1. Calculations are performed with $\beta = 0.5$, $r_m = 0.03$ μm, $\sigma_d = 2.1$ (according to (2.12), $k_{s0} = 1.44$), $b = 0.25$ (ammonium sulfate and solubility 50%) and 3 values of $w = 3.5$, 21 and 101 cm s^{-1}. As seen in Fig. 1, the left-hand side (which is just t_m) begins at zero and linearly grows with time, while the right-hand side of (4.12) begins at nonzero values and grows almost linearly but much slower. Thus, the right- and left-hand sides should intersect at some point t, which is a solution of (4.12) for t_m, 38.7, 14.9, and 6.9 seconds respectively for these values of w. Then, with known t_m, we can calculate s_m using (4.4), and N_{dr} using the algebraic law (4.16) or generalized power law (4.17).

To check the consistency of this solution, we compare this method with two methods from Abdul-Razzak et al. (1998, hereafter AGC): their parameterization and detailed calculations based on the parcel model runs. Calculations were made using the same parameters as in Fig. 1 in

AGC: at T = 10 ºC, p = 800 mbar, and updraft w = 5 m s^{-1}. Aerosol consists of fully soluble ammonium sulfate particles, the size spectrum is lognormal with r_{d0} varied in the range indicated on x-axis, dispersion σ_d = 2.5, total concentration N_a = 200 cm^{-3}. Shown in Fig. 2a is the fraction activated, N_{dr}/N_a, as a function of the mean geometric radius r_{d0} varied in the range 0.001 - 0.1 μm, calculated with the modified power law (4.17) and with the two methods from AGC. Fig. 2a shows that the curve obtained from (4.17; labeled KC) is close to those from AGC; the precise AGC parcel results lie between the parameterizations AGC and KC.

Fig. 2b shows the differences between the methods calculated as $(x_1 - x_2)/x_2 \times 100$, where x_1 and x_2 and represent each compared pair of results. One can see that the difference between the methods does not exceed 10 % for realistic spectra at $r_{d0} \geq 0.01$ μm and 5 % at $r_{d0} \geq 0.03$ μm. The errors increase toward smaller values of r_{d0}, mostly because the fraction N_{dr}/N_a (denominator x_2) becomes small, but these results are shown rather for illustration, and size spectra with small $r_{d0} <$ 0.01 μm play little role in drop activation. Thus, the method developed here is in a good agreement with both methods from AGC, despite their completely different mathematical formulations.

5. Calculations of CCN activation kinetics

A series of calculations is performed using (4.12) - (4.17) to study various characteristics of CCN activation kinetics with varying vertical velocity. The effects of variations of any other single parameter of the set (r_m, σ_d, N_a, b, α_c) are studied by varying this parameter while the others were fixed as described below. The results shown in Figures 3-7 are obtained with the condensation coefficient α_c = 1, and the effect of variations of α_c is shown in Figs. 8, 9.

Fig. 3 demonstrates the effect of variations of the modal radius r_m on the kinetics of drop activation. The maximum time t_m (Fig. 3a) decreases with increasing w from 50 -150 s and with increasing r_m (which diminishes with increasing w). The maximum supersaturation s_m (Fig. 3b)

increases from 0.02 - 0.08 % at $w = 1$ cm s^{-1} to 1-1.5 % s at $w = 5$ m s^{-1}, and decreases with increasing r_m. Both t_m and s_m when plotted versus w in double-log coordinates show nearly straight lines with slightly changing slopes. The droplet concentrations and fraction activated (Fig. 3c,d) increase with increasing w and r_m, and roughly resemble smoothed Heaviside step functions (KC06). Note that N_{dr} is limited by N_a, in contrast to the usual power law expression.

The indices $k(w)$ (or $k(s_m)$) of the generalized power law (4.17) substantially decrease with increasing w (Fig. 3e), from 1.5-1.8 at small values of w to 0.4 and values close to zero at w = 5 m s^{-1}. The indices $k(s_m)$ decrease with increasing values of r_m. The coefficients $C(s_m)$ also decrease with w from 10^3 - 2×10^4 cm^{-3} at small w to values ~ N_a at $w >$ 1-2 m s^{-1} (Fig. 3f); variations of $C(s_m)$ are much smaller at smaller values of r_m. These 2 Figures (3e,f) for k and C may provide a physical basis for the C-k space of drop activation suggested by Braham (1976) based on generalization of experimental data. However, the consideration here shows that this space is actually multidimensional since $N_{dr}(w)$ depends also on several other parameters. The method developed here allows calculation of C and k for any given w and any fixed set of aerosol microphysical parameters (r_m, σ_d, N_a, b, α_c) that together with w form a 6-dimensional C-k space, or together with the temperature T and surface tension ζ form an 8-dimensional space.

The values of the integral $J_0(w) = r_{act}(w)$ defined in (3.14) and shown in Fig. 4a increase from 0.04 - 0.2 μm at small values of w to 1-2 μm at large values of w and increase with increasing values of r_m. The relaxation time $\tau_{p,ac}$ during activation calculated with (3.13) decreases from ~ 70 seconds at $w = 1$ cm s^{-1} to 4 - 10 seconds at $w \geq 0.3$ m s^{-1}. The latter value of $\tau_{p,ac}$ is quite comparable to the drop relaxation time in a developed cloud, i.e., the rate of vapor absorption by the newly formed drops is comparable to that of the "old" drops.

An important characteristic of the increase in CCN radii during activation is the ratio $r_{act}(w)/r_m$. It is actually this characteristic that was used in Abdul-Razzak et al. (1998), Abdul-Razzak and Ghan (2000), Fountoukis and Nenes (2005) and others when developing approximate

parameterizations of drop activation. Fig. 4b shows that $r_{act}(w)/r_m$ increases from 1-4 at $w = 1$ cm s^{-1} to the values ≥ 10 at $w \geq 0.2$ - 0.4 m s^{-1}, i.e., this ratio is >> 1 at the typical turbulent updrafts in Sc clouds and vertical velocities in cumulus clouds. Fig. 4c shows that the integral $J_3 < 1$ and decreases with increasing w and r_m. The depth of the activation layer calculated as $H_{act} = wt_m$ (Fig. 4d) increases from less than 1 m at small values of w to 20-25 m at large values of w, i.e., activation occurs within 1 typical grid box of ~ 50 m of a LES model and may occupy more levels in models with finer resolution. Recall, these results were obtained with $\alpha_c = 1$, and H_{act} is greater for smaller values of α_c as described below.

The effect of varying size dispersion σ_d is shown in Fig. 5a-f. The dependencies on w for all values of σ_d are the same as described above. An increase in σ_d (broadening of the CCN size spectra) is most pronounced at small values of w, where it shortens activation time t_m, reduces maximum supersaturation, index $k(s_m)$ and coefficient $C(s_m)$, and causes increase in droplet concentration and fraction activated. The effect of σ_d decreases at $w > 1$ m s^{-1} and almost vanishes at $w > 2$ m s^{-1}, i.e., the width of the size spectra becomes much less significant in the large updrafts in convective clouds.

Fig. 6 depicts the effect of variations of CCN concentration N_a in the range 100 cm^{-3} (e.g., maritime or arctic clouds) to 2000 cm^{-3} (continental or moderately polluted atmosphere). A 20-fold increase in N_a causes a decrease in t_m and s_m by 2.5 times at small values of w and 4.5 times at large values of w (Fig. 6a), i.e., the effect is smaller than linear, and increases with w. The drop concentration increases with N_a but much slower than linearly, so that fraction activated decreases with increasing N_a; this decrease is greater at moderate values of w on the order of turbulent fluctuations ~ 0.3-0.5 m s^{-1}, and smaller at small and large values of w (Fig. 6c,d). Both the index $k(w)$ and coefficient $C(w)$ substantially increase at larger values of N_a, and their variations are also maximum at moderate values of w.

Effect of variations of soluble fraction ε_v of ammonium sulfate from fully soluble nuclei with ε_v = 100 % to 6 % is shown in Fig. 7. The values of b calculated from (2.5) for the soluble fraction proportional to the volume ($\beta = 0.5$) are ≈ 0.5 and 0.03 respectively. The effect of solubility is nonlinear in w: it decreases with increasing w. A more than 16-fold decrease in soluble fraction leads to the decrease in t_m and s_m by only a factor of two at small w, this difference further decreases with increasing w, and becomes almost negligible at w = 5 m s^{-1}. With this 16-fold decrease in ε_v, the drop concentration and fraction activated decrease by a factor of 3.5 at small w, a factor of 2-2.5 at w = 0.2 - 1 m s^{-1} (turbulent fluctuations), and this difference is only 15-20 % at w = 4-5 m s^{-1} (convective clouds). The value for convective clouds with large updrafts is close to that in Abdul-Razzak et al. (1998). Fig. 7 shows the effect of solubility in the wide range of w and its increase at smaller w, i.e., indicates that solubility of CCN may play much more important effect in stratiform than in convective cloud types. The index $k(w)$ increases and the coefficient $C(w)$ decreases for lower solubility. An interesting feature of activation is that even the CCN with very small solubility can serve as effective nuclei for drop activation.

The results presented in Figs 3-7 were obtained with the condensation coefficient $\alpha_c = 1$ that may correspond to drops of pure water (PK97). The values of α_c in the range 1 to 0.001 and smaller have been measured in various experiments (e.g., PK97, Table 5.4); α_c may become smaller than 10^{-3} to 10^{-5} in the presence of surfactants and organic substances at the CCN surface (PK97, Charlson et al. 2001, Feingold and Chuang 2002; Chuang 2003; a review of earlier theoretical, laboratory and filed studies is given in Buikov and Khvorostyanov 1979). To study the effects of α_c, we tested 5 values, $\alpha_c = 10^{10}$, 1, 0.1, 0.04, 0.01. The corresponding kinetic corrections ξ in dr/dt in (3.5a,b) can be written for the standard conditions as $\xi \approx 0.15/\alpha_c$ μm, and for these 5 cases are respectively 0; 0.15; 1.5; 3.8; and 15 μm. (The real value of α_c is of course always ≤ 1, but the choice $\alpha_c = 10^{10}$ allows to study the case with $\xi = 0$ used in some works).

The impacts of varying the condensation coefficient α_c are shown in Figs. 8, 9. The difference in t_m and s_m and in all the other characteristics shown in Figs. 8, 9 for the case $\alpha_c = 10^{10}$ (absence of kinetic correction) and $\alpha_c = 1$ generally does not exceed 4-7 %. That is, the case $\alpha_c = 1$ considered in the parameterizations by Abdul-Razzak et al. (1998), Abdul-Razzak and Ghan (2000), Nenes and Seinfeld (2003) and in Figs 3-7 here is close to the absence of the kinetic correction as in Twomey (1959) and subsequent similar parameterizations. A decrease in α_c from 1 to 0.1 causes an increase in t_m and s_m of 50-70 %; the droplet concentration and fraction activated are almost twice as large at small values of w with a gradual decrease of the difference toward larger values of w. Both the index $k(w)$ and coefficient $C(w)$ decrease but in such a way that N_{dr} increases. A decrease in α_c from 1 to 0.04 (typical values used in many cloud models) results in 2-2.5-fold increase in t_m, s_m; corresponding increase in N_{dr} is 1.5 - 2 times at w = 10-50 cm s^{-1} (comparable or greater than the indirect aerosol effect), and gradually vanishes at large w. When α_c decreases from 1 to 0.01, this causes 5-6- fold increase in t_m, s_m; this leads to an increase in N_{dr} by 100 - 50 % at w = 10-50 cm s^{-1}, which tends to zero at large w. Any decrease in α_c is accompanied by a significant decrease in $k(w)$ and $C(w)$ similar to those just described (Fig. 8a-f).

The values of $r_{act}(w) = J_0(w)$ and r_{act}/r_m become much smaller with decreasing α_c (Fig. 9), and the assumption $r_{act}/r_m >> 1$ with $\alpha_c \le 0.04$ made in some previous works on drop activation is not satisfied even for sufficiently high values of w. The quantity r_{act}/r_m characterizes the ratio $r_{act}/r_d(t,t_0)$, and the assumption $r_{act}/r_d(t,t_0) >> 1$ was implicit in Twomey (1959), and similar parameterizations in evaluation of the integral $J_0(w)$. The height of activation substantially increases for small $\alpha_c \le 0.1$ (Fig. 9d), and may exceed 30-100 m, so that the process of activation should be distributed among several levels in models with fine vertical resolution.

Thus, a decrease in the condensation coefficient leads to slower CCN activation, and higher maximum supersaturation, droplet concentration, and fraction activated. The magnitude of these variations can be higher than possible direct or indirect aerosol effects on climate change;

that is, uncertainties in α_c may prevent correct estimates of anthropogenic effects on climate. Thus, correct measurements of the condensation coefficient and use of its proper values for evaluation of the concentration of activated drops is very important. The method developed here allows direct calculations of CCN activation in a model or compilation of lookup tables for cloud and climate models for any values of condensation coefficient.

6. Conclusions

A simple yet consistent model of cloud drops activation on CCN with lognormal or equivalent algebraic size spectrum is developed. An integro-differential equation for the integral water supersaturation in a cloud is derived and analyzed. Based on the equivalence of the lognormal and algebraic aerosol size spectra and CCN differential activity spectra, and solving the supersaturation equation with the algebraic activity spectrum, analytical expressions are obtained for the time t_m of CCN activation process, the maximum supersaturation s_m, and droplet concentration N_{dr} limited by the total aerosol concentration at high supersaturations. All three quantities are expressed as functions of the vertical velocity w, and characteristics of the CCN size spectra: mean geometric radius r_{d0}, dispersion σ_d, and parameter of solubility b.

A generalized power law for the drop activation, $N_{dr}(s_m) = C(s_m)s_m^{k(s_m)}$, is formulated that is similar to the Twomey's power law, but both the coefficient $C(s_m)$ and index $k(s_m)$ are functions of supersaturation. These functions are expressed analytically via vertical velocities and CCN microphysical parameters. Both $C(s_m)$ and $k(s_m)$ are decreasing functions of s_m or w, which has been observed (e.g., Yum and Hudson 2001 and review therein) but hitherto unexplained.

The analytical expressions derived here and examples of calculations show that these parameters also decrease with increasing vertical velocities, but can increase or decrease with variations of the aerosol microphysical parameters. Since the work of Twomey (1959), for almost 5 decades, there has been a continued search for the best value of k and of C or for 2-4 values that

can be representative over the whole supersaturation range (see e.g., reviews in Jiusto and Lala 1981; Hegg and Hobbs 1992; PK97; Seinfeld and Pandis 1998). The equations derived in KC06, KC07 and here show that unique values of k and C cannot exist: there is infinite number of $k(s_m)$ and of $C(s_m)$ as continuous functions of s_m or w, but they are simply expressed here via aerosol microstructure; for a given microstructure, they are decreasing functions of vertical velocity.

A simple and economical numerical solution of the integral supersaturation equation is described that does not require running parcel models. An extended series of numerical experiments was performed, in which the dependencies of the time t_m, supersaturation s_m, drop concentration N_{dr}, fractions activated, coefficient $C(s_m)$, index $k(s_m)$, and several other important characteristics of activation process were studied as functions of vertical velocity and the aerosol physico-chemical properties.

The results of this study have highlighted the sensitivity of the nucleation process to the water condensation coefficient α_c. Many previous parameterizations of CCN activation have not included variations of α_c. The method developed here allows studying effects of variations of α_c without running parcel models and retuning the coefficients of parameterization. It was shown that the assumptions of Twomey (1959) (neglecting the kinetic correction ξ in the drop growth rate, which is equivalent to $\alpha_c = \infty$) yields results close to those obtained in Abdul-Razzak et al. (1998), Abdul-Razzak and Ghan (2000) with $\alpha_c = 1$, which can be characteristic of pure water drops. A decrease in the condensation coefficient to 0.04-0.01, which may be characteristic of polluted cloud drops, leads to a 2.5-6 -fold increase of the activation time t_m and maximum supersaturation s_m. This results in an increase in the concentration of activated drops by 50-270 % at vertical velocities $w \sim 0.1$ - 0.5 m s^{-1}, typical for turbulent fluctuations, and by 10 - 6 % at $w \sim$ 2-3 m s^{-1}, typical of convective clouds; the effect decreases with increasing w.

Our results on increasing N_{dr} with decreasing α_c are in qualitative agreement with parcel model simulations given in Nenes et al. (2002), and simulations and parameterization in Ming et

al. (2006) at $w \sim 1$ m s^{-1}. Note that we assume here the same value of α_c for the whole CCN and drops size spectra, consider only moderate variations of α_c as those measured in various experiments (PK97, Table 5.4) and used in cloud models. We do not consider more complicated processes like formation of surfactant organic films with much smaller values $\alpha_c \sim 10^{-5}$, and breaking the films in the fraction of the largest drops with corresponding increase in α_c to 0.04, as, e.g., in Buikov and Khvorostyanov (1979), Feingold and Chuang (2002), Nenes et al. (2002).

The values of α_c in the range 0.04 - 1 are typically used in cloud models and parameterizations. There is currently no complete clarity on the reasons for the measured variations of α_c, and there is not a common consensus on its best value, but it is usually hypothesized that the lower values of α_c may be caused by the presence of impurities in the drops, and is characteristic of polluted clouds (PK97, Seinfeld and Pandis 1998). The results of this work indicate that the clouds polluted with any substance that lowers α_c to 0.01-0.04, but does not cause strong absorption of solar radiation (without substantial presence of soot), may have notably higher albedo and lower precipitation than clouds of pure drops with $\alpha_c \sim 1$.

In contrast to the known "first indirect aerosol effect" (albedo increase or Twomey (1977) effect) and "second indirect aerosol effect" (precipitation decrease or Albrecht (1989) effect) due to increase of aerosol concentration, these albedo and precipitation effects may occur without increased aerosol concentration, due to chemical processing of the existing CCN or presence of the corresponding chemicals during CCN and drops formation (e.g., Laaksonen et al. 1998; McFiggans et al. 2006), which may change α_c. This conclusion about chemical amplification of the indirect aerosol effects is in agreement with parcel model results and other parameterizations (e.g., Nenes et al. 2002, Rissman et al. 2004). Note that we considered here only one case with variations of α_c, and all the other aerosol parameters fixed, but the method developed here allows for examination of effects of α_c for various aerosol types in cloud and climate models. Variations of the surface tension due to surface-active organic solutes that may

further increase albedo (Facchini et al. 1999; Charlson et al. 2001; Rissman et al. 2004), can be also accounted for in this method by appropriate modification of the Kelvin parameter introduced in section 2.

Since the algebraic size and CCN activity spectra derived in KC06, KC07 and selected in this work are equivalent to the lognormal spectra, our generalized power law model is analogous to the lognormal approach developed in Ghan et al. (1993, 1995), von der Emde and Wacker (1993), Abdul-Razzak et al. (1998, 2000), Fountoukis and Nenes (2005). However, the algebraic representation of the size spectra has several advantages.

1) While the lognormal functions are a convenient fit to the observed spectra, they generally do not have a physical justification. By contrast, the algebraic spectra have such a justification: they are the interpolation among several spectral sub-ranges, each of which is a power law (direct with positive index or Junge-type inverse with negative index), and can be obtained as the solutions to the aerosol coagulation equation with sources and sinks (e.g., Junge 1963; Lushnikov and Smirnov 1975; Lushnikov and Piskunov 1977; Voloshchuk 1984; PK97, Seinfeld and Pandis 1998). This allows direct expression of the size spectra via the primary kinetic parameters of aerosol formation processes (gas-to-particle conversion and coagulation): first, the modal radius and dispersion of the CCN size spectra, and then, all the other parameters of CCN activity spectra and drop concentration.

2) The algebraic size spectra in r-space convert to the algebraic CCN differential activity spectra in s-space, the integrals of which are simpler to evaluate analytically. Analytical expressions for t_m, s_m and N_{dr} will be presented in the following paper.

These numerical and analytical solutions and expressions for the parameters presented here can be used in several different ways for developing parameterizations of the drop activation process for cloud and climate models. Since the method developed here is based on direct solution of the integral supersaturation equation, it does not require running a parcel model and is computationally more efficient and flexible, and can be used for tuning parameters of the recently

developed analytical parameterizations, for calculating lookup tables for drop activation that could be used in the cloud and climate models. Besides, it can be used for estimating cloud drop spectral dispersions and the indirect dispersion effect on climate, as, e.g., in Liu et al. (2006), Peng and Lohmann (2003).

Acknowledgments. This research has been supported by the DOE Atmospheric Radiation Measurement Program and NASA Modeling and Parameterization Program. The authors are grateful to the three anonymous reviewers for useful remarks that helped to clarify and improve the text. Jody Norman is thanked for help in preparing the manuscript.

References

Abdul-Razzak, H., S. J. Ghan, and C. Rivera-Carpio, 1998: A parameterization of aerosol activation: 1. Single aerosol type, *J. Geophys. Res.,* **103***,* 6123–6131.

_____, and S. J. Ghan, 2000: A parameterization of aerosol activation: 2. Multiple aerosol types, *J. Geophys. Res.,* **105,** 6837–6844.

Albrecht, B., Aerosols, cloud microphysics and fractional cloudiness, 1989: *Science,* **245,** 1227-1230.

Bauer, S. E. and D. Koch, 2005: Impact of heterogeneous sulfate formation at mineral dust surfaces on aerosol loads and radiative forcing in the Goddard Institute for Space Studies general circulation model. *J. Geophys. Res.,* **110**, http://dx.doi.org/10.1029/2005JD005870.

Braham, R. R., 1976: CCN spectra in *C-k* space *J. Atmos. Sci.,* **33**, 343-346.

Buikov, M. V., 1966: Kinetics of heterogeneous condensation at adiabatic cooling. Part 2: Kinetic regime of droplet growth. *Colloid. J.,* **28** (5), 635-639.

Buikov, M. V., and V. I. Khvorostyanov, 1979: Fog dispersal with surface-active reagents. A Review. *Sov. Meteorol. Hydrol.*, No 5, 57-68 (English Translation by Allerton Press).

Charlson, R.J., J. H. Seinfeld, A. Nenes, M. Kulmala, A. Laaksonen, and M. C. Facchini, 2001: Reshaping the theory of cloud formation, *Science*, **292**, 20205-2026.

Cohard, J.-M., J.-P. Pinty, and C. Bedos, 1998: Extending Twomey's analytical estimate of nucleated cloud droplet concentrations from CCN spectra. *J. Atmos. Sci*., **55***,* 3348–3357.

_____, J.-P. Pinty, and K. Suhre, 2000: On the parameterization of activation spectra from cloud condensation nuclei microphysical properties. *J. Geophys. Res., 105* (D9), 11753–11766.

Chuang, P., 2003: Measurement of timescale of hygroscopic growth for atmospheric aerosols. *J. Geophys. Res.*, **108**(D9), 4283, doi:10.1029/2002JD002757.

Curry, J. A., and P. J. Webster, 1999: *Thermodynamics of Atmospheres and Oceans,* Academic Press, London, 467 pp.

Facchini, M., M. Mircea, S. Fuzzi, and R. Charlson, 1999: Cloud albedo enhancement by surface-active organic solutes in growing droplets. *Nature*, **401**, 257-259.

Feingold, G., and P. Chuang, 2002: Analysis of the influence of film-forming compounds on droplet growth: Implications for cloud microphysical processes and climate. *J. Atmos. Sci.,* **59**, 2006-2018.

Fountoukis, C, and A. Nenes, 2005: Continued development of a cloud droplet formation parameterization for global climate models, *J. Geophys. Res.,* **110**, D11212, doi:10.1029/2004JD005591.

Fuchs, N., 1959: *Evaporation and Droplet Growth in Gaseous Media*. Pergamon Press, 91 pp.

Ghan, S., C. Chuang, and J. Penner, 1993: A parameterization of cloud droplet nucleation. Part 1, Single aerosol species, *Atmos. Res.,* **30,** 197-222.

_____, C. Chuang, R. Easter, and J. Penner, 1995: A parameterization of cloud droplet nucleation. 2, Multiple aerosol types, *Atmos. Res.,* **36***,* 39-54.

_____, L. Leung, R. Easter, and H. Abdul-Razzak, 1997: Prediction of cloud droplet number in a general circulation model, *J. Geophys. Res.,* **102**, 777-794,

Gradshteyn, I. S., and I. M. Ryzhik, 1994: *Tables of Integrals, Series, and Products*, 5th ed., A. Jeffery, Ed., Academic Press, 1204 pp.

Hegg, D. A., and P. V. Hobbs, 1992: Cloud condensation nuclei in the marine atmosphere: A review. *Nucleation and Atmospheric Aerosols,* N. Fukuta and P. E. Wagner, Eds., A. Deepak, Hampton, Virginia, 181-192.

Ji, Q., and G. E. Shaw, 1998: On supersaturation spectrum and size distribution of cloud condensation nuclei. *Geophys. Res. Lett.,* **25***,* 1903-1906.

Jiusto, J. E., and G. G. Lala, 1981: CCN-supersaturation spectra slopes (*k*). *J. Rech. Atmos.,* **15**, 303-311.

Junge, C. E., 1963: *Air Chemistry and Radioactivity.* Academic Press, New York and London, 424 pp.

Khvorostyanov, V. I., and J. A. Curry, 1999: A simple analytical model of aerosol properties with account for hygroscopic growth. Part I: Equilibrium size spectra and CCN activity spectra, *J. Geophys. Res*., **104** (D2), 2163-2174.

_____, and _____, 2005: The theory of ice nucleation by heterogeneous freezing of deliquescent mixed CCN. Part 2: Parcel model simulation. *J. Atmos. Sci.,* **62**, No 2, 261-285

_____, and _____, 2006: Aerosol size spectra and CCN activity spectra: Reconciling the lognormal, algebraic and power laws, *J. Geophys. Res.,* **111** (D12202), doi:10.1029/2005JD006532.

_____, and _____, 2007: Refinements to the Köhler's theory of aerosol equilibrium radii, size spectra, and droplet activation: Effects of humidity and insoluble fraction. *J. Geophys. Res.,* **112**, D5 (D05206). http://dx.doi.org/10.1029/2006JD007672.

Kreidenweis, S. M., K. Koehler, P. J. DeMott, A. P. Prenni, C. Carrico, and B. Ervens, 2005: Water activity and activation diameters from hygroscopicity data - Part I: Theory and application to inorganic salts, *Atmos. Chem. Physics,* **5**, 1357-1370.

Laaksonen, A., P. Korhonen, M. Kulmala, and R. J. Charlson, 1998: Modification of the Köhler equation to include soluble trace gases and slightly soluble substances, *J. Atmos. Sci.,* **55**, 853-862.

Levin, L. M. and Y. S. Sedunov, 1966: A theoretical model of condensation nuclei. The mechanism of cloud formation in clouds, *J. Rech. Atmos.,* **2** (2-3), 45 - 56.

Levin, Z., E. Ganor, and V. Gladstein, 1996: The effects of desert particles coated with sulfate on rain formation in the Eastern Mediterranean, *J. Appl. Meteorol.,* **35**, 1511–1523.

Liu, Y., P. H. Daum, and S. S. Yum, 2006: Analytical expression for the relative dispersion of the cloud droplet size distribution. *Geophys. Res. Lett.,* **33**, L02810, doi:10.1029/2005GL024052.

Lohmann, U., J. Feichter, C. C. Chuang, and J. E. Penner, 1999: Predicting the number of cloud droplets in the ECHAM GCM, *J. Geophys. Res.,* **104**, 9169-9198.

Lushnikov, A. A., and V. I. Smirnov, 1975: Stationary coagulation and size distributions of atmospheric aerosols. *Izv. Acad Sci. USSR, Phys. Atmos. Ocean*, **11** (2**)**, 139-151.

_____, and V. N. Piskunov, 1977: Formation of stationary distributions in the coagulating systems with decaying particles. *Colloid J*., **5**, 857-862.

McFiggans, G., P. Artaxo, U. Baltensperger, H. Coe, M. C. Facchini, G. Feingold, S. Fuzzi, M. Gysel, A. Laaksonen, U. Lohmann, T. F. Mentel, D. M. Murphy, C. D. O'Dowd, J. L. Snider, and E. Weingartner, 2006: The effect of physical and chemical aerosol properties on warm cloud droplet activation. *Atmos. Chem. Phys.,* **6**,. 2593-2649.

Ming, Y., V. Ramaswamy, L. J. Donner, and V. T. J. Phillips, 2006: A new parameterization of cloud droplet activation applicable to general circulation models. *J. Atmos. Sci.,* **63**, 1348-1356.

Morrison, H., and W. W. Grabowski, 2007. Comparison of bulk and bin warm rain microphysics models using a kinematic framework. *J. Atmos. Sci.,* **64**, 2839 - 2861.

_____, J. A. Curry, and V. I. Khvorostyanov, 2005a: A new double-moment microphysics parameterization for application in cloud and climate models, Part 1: Description. *J. Atmos. Sci.*, **62**, 1665-1677.

_____, J. A. Curry, M. D. Shupe, and P. Zuidema, 2005b: A new double-moment microphysics scheme for application in cloud and climate models, Part 2: Single-column modeling of arctic clouds. *J. Atmos. Sci*., **62**, 1678-1693.

Nenes, A., and J. H. Seinfeld, 2003: Parameterization of cloud droplet formation in global climate

models, *J. Geophys. Res.,* **108,** 4415, doi:10.1029/2002JD002911.

_____, R. J. Charlson, M. C. Facchini, M. Kulmala, A. Laaksonen, and J. H. Seinfeld, 2002: Can chemical effects on cloud droplet number rival the first indirect effect? *Geophys. Res. Lett.*, **29** (17), 1848, doi: 10.1029/2002GL015295.

Peng, Y., and U. Lohmann, 2003: Sensitivity study of the spectral dispersion of the cloud droplet size distribution on the indirect aerosol effect. *Geophys. Res. Lett.,* **30** (10), 1507.

Pruppacher, H. R. and J. D. Klett, 1997: *Microphysics of Clouds and Precipitation*, 2nd ed., Kluwer Academic Publishers: Boston, MA, 954 pp.

Rissman, T. A., A. Nenes, and J. H. Seinfeld, 2004: Chemical amplification (or dampening) of the Twomey effect: Conditions derived from droplet activation theory, *J. Atmos. Sci.,* **61***,* 919-930.

Saleeby, M. S., and W. R. Cotton, 2004: A large-droplet mode and prognostic number concentration of cloud droplets in the Colorado State University regional atmospheric modeling system (rams). Part I: module descriptions and supercell test simulations. *J. Appl. Meteorol.,* **43***,* 182-195.

Sedunov, Y. S. 1967: Kinetics of the initial stage of droplet growth in clouds. *Izv. Acad. Sci. USSR, Atmos. Ocean. Phys.*, **3** (1), 37-48.

Sedunov, Y. S., 1974: *Physics of Drop Formation in the Atmosphere*, Wiley, New York, 234 pp.

Seinfeld, J. H., and S. N. Pandis, 1998: *Atmospheric Chemistry and Physics*, Wiley, New York, 1326 pp.

Svenningsson, B., J. Rissler, E. Swietlicki, M. Mircea, M. Bilde, M. C. Facchini, S. Decesari, S. Fuzzi, J. Zhou, J. Mønster, and T. Rosenørn, 2006: Hygroscopic growth and critical supersaturations for mixed aerosol particles of inorganic and organic compounds of atmospheric relevance. *Atmos. Chem. Phys.,* **6**, 1937-1952.

Twomey, S., The nuclei of natural cloud formation. II. 1959: The supersaturation in natural clouds and the variation of cloud droplet concentration. *Geoph. Pura Appl*., **43**, 243-249.

_____, 1977: *Atmospheric Aerosols,* Elsevier, New York, 302 pp.

von der Emde, K., and U. Wacker, 1993: Comments on the relationship between aerosol size spectra, equilibrium drop size spectra and CCN spectra. *Contrib. Atmos., Phys.,* **66**, 157-162.

Wurzler, S., T. G. Reisin, and Z. Levin, 2000: Modification of mineral dust particles by cloud processing and subsequent effect on drop size distributions, *J. Geophys. Res.,* **105** (D4), 4501-4512.

Figure captions

Fig. 1. Illustration of the method of solution of the equation (4.12) for t_m. The left hand side (LHS), time, is denoted by the solid squares. The right hand side (RHS) is calculated with r_m = 0.03 μm, σ_d =2.1, β = 0.5, b = 0.25 and 3 values of w = 3.5, 21 and 101 cm s^{-1}, as indicated in the legend. The intersections of the RHS and LHS, marked with the ellipses, are the solutions for t_m, here, respectively, 38.7, 14.9, 6.9 seconds.

Fig. 2. Comparison of the fraction activated as a function of the mean geometric radius r_{d0} calculated with the modified power law of this work (KC) with parameterization from Abdul-Razzak et al. (1998) (AGC) and with results of detailed parcel simulations from AGC (parcel). (a) fraction activated, N_{dr}/N_a; and (b) relative errors in percent between each two methods as indicated in the legend. Calculations are made at T = 10 ºC, p = 800 mbar, and updraft of 5 m s^{-1}. Aerosol consists of fully soluble ammonium sulfate particles, the size spectrum is lognormal with r_{d0} varied in the range indicated on x-axis, dispersion σ_d = 2.5, total concentration N_a = 200 cm^{-3}. The error between the methods does not exceed 10 % for realistic spectra at $r_{d0} \geq 0.01$ μm and 5 % at $r_{d0} \geq 0.03$ μm.

Fig. 3. Effect of variations of the modal radius r_m indicated in the legend. (a) maximum time t_m, sec; (b) supersaturation s_m, %; (c) droplet concentration N_{dr}, cm^{-3}; (d) fraction activated; (e), index $k(s_m)$; (f) coefficient $C_{cp}(s_m)$, cm^{-3} as functions of vertical velocity w calculated with KC06 CCN activity spectrum. Size dispersion σ_d = 1.8; β = 0.5 (volume soluble fraction), b = 0.25 (50 % of ammonium sulfate), CCN concentration is N_a = 500 cm^{-3}.

Fig. 4. Additional characteristics of activation. (a) effective radius of activation r_{act} (integral J_0); (b) ratio r_{act}/r_m; (c) Integral J_3; (d) height of activation H_{lift}; input parameters are the same as in Fig. 3.

Fig. 5. Effect of variations of size dispersion σ_d indicated in the legend. (a) maximum time t_m, sec; (b) supersaturation s_m, %; (c) droplet concentration N_{dr}, cm^{-3}; (d) fraction activated; (e), index $k(s_m)$; (f) coefficient $C_{cp}(s_m)$, cm^{-3} as functions of vertical velocity w calculated with KC06 CCN activity spectrum. The mean geometric radius $r_{d0} = 0.05$ μm, $\beta = 0.5$ (volume soluble fraction), $b = 0.25$ (50 % of ammonium sulfate), CCN concentration is $N_a = 500$ cm^{-3}.

Fig. 6. Effect of variations of CCN concentration N_a indicated in the legend. (a) maximum time t_m, sec; (b) supersaturation s_m, %; (c) droplet concentration N_{dr}, cm^{-3}; (d) fraction activated; (e), index $k(s_m)$; (f) coefficient $C_{cp}(s_m)$, cm^{-3} as functions of vertical velocity w calculated with KC06 CCN activity spectrum. The mean geometric radius $r_{d0} = 0.05$ μm, $\sigma_d = 1.8$, $\beta = 0.5$ (volume soluble fraction), $b = 0.25$ (50 % of ammonium sulfate).

Fig. 7. Effect of variations of soluble fraction ε_v of ammonium sulfate from 6 % to fully soluble nuclei (100 %) indicated in the legend. (a) maximum time t_m, sec; (b) supersaturation s_m, %; (c) droplet concentration N_{dr}, cm^{-3}; (d) fraction activated; (e), index $k(s_m)$; (f) coefficient $C_{cp}(s_m)$, cm^{-3} as functions of vertical velocity w calculated with KC06 CCN activity spectrum. The mean geometric radius $r_{d0} = 0.05$ μm, $\sigma_d = 1.8$, $\beta = 0.5$ (volume soluble fraction), $N_a = 500$ cm^{-3}.

Fig. 8. Effect of variations of condensation coefficient α_c indicated in the legend ($\alpha_c = 10^{10}$ corresponds to $\xi = 0$). (a) maximum time t_m, sec; (b) supersaturation s_m, %; (c) droplet concentration N_{dr}, cm^{-3}; (d) fraction activated; (e), index $k(s_m)$; (f) coefficient $C_{cp}(s_m)$, cm^{-3} as

functions of vertical velocity w calculated with KC06 CCN activity spectrum. The mean geometric radius r_{d0} = 0.05 μm, σ_d = 1.8, β = 0.5 (volume soluble fraction), b = 0.25 (50 % of ammonium sulfate), CCN concentration is N_a = 500 cm^{-3}.

Fig. 9. Effect of variations of condensation coefficient α_c indicated in the legend, continued (α_c = 10^{10} corresponds to ξ = 0). (a) effective radius of activation r_{act} (integral J_0); (b) ratio r_{act}/r_m; (c) Integral J_3; (d) height of activation H_{lift}; input parameters are the same as in Fig. 8.

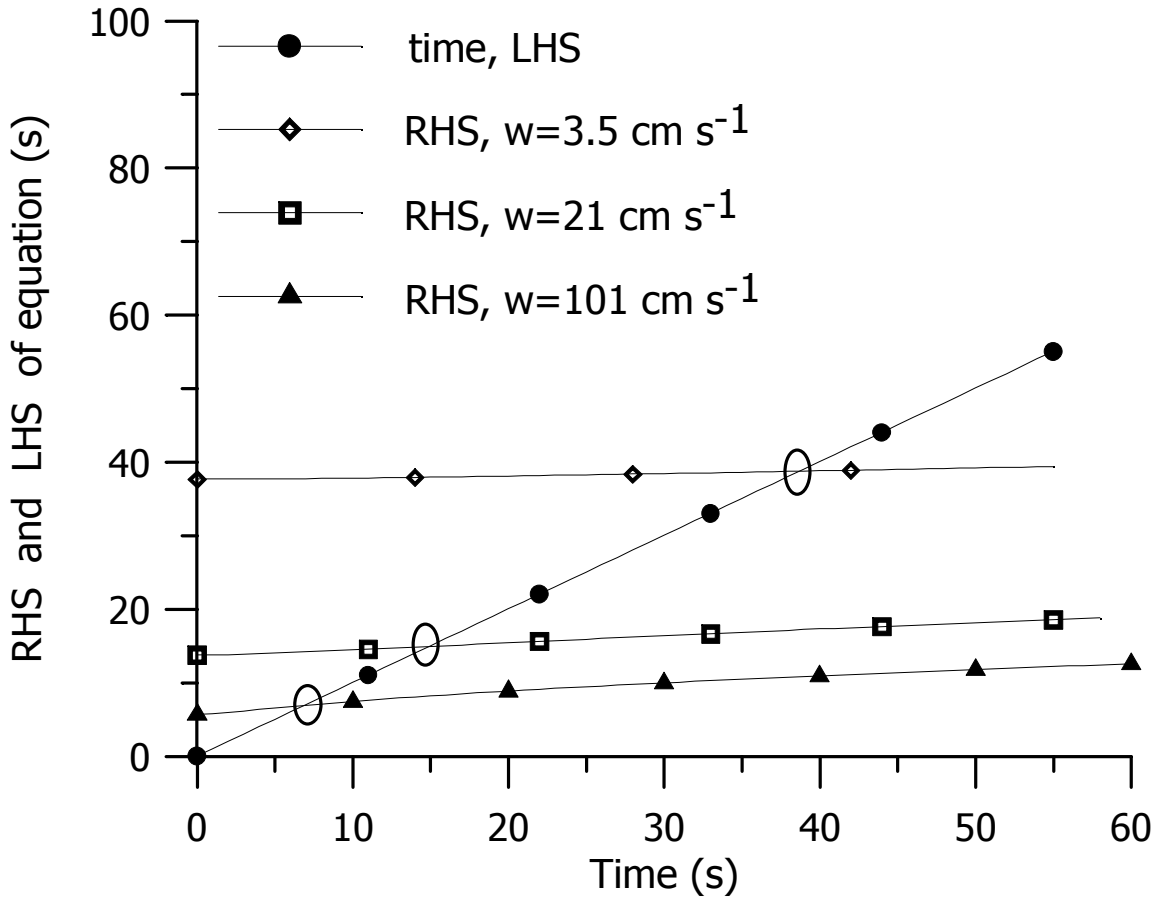

Fig. 1. Illustration of the method of solution of the equation (4.12) for t_m. The left hand side (LHS), time, is denoted by the solid circles. The right hand side (RHS) is calculated with r_m = 0.03 μm, σ_d =2.1, β = 0.5, b = 0.25 and 3 values of w = 3.5, 21 and 101 cm s^{-1}, as indicated in the legend. The intersections of the RHS and LHS, marked with the ellipses, are the solutions for t_m, here, respectively, 38.7, 14.9, 6.9 seconds.

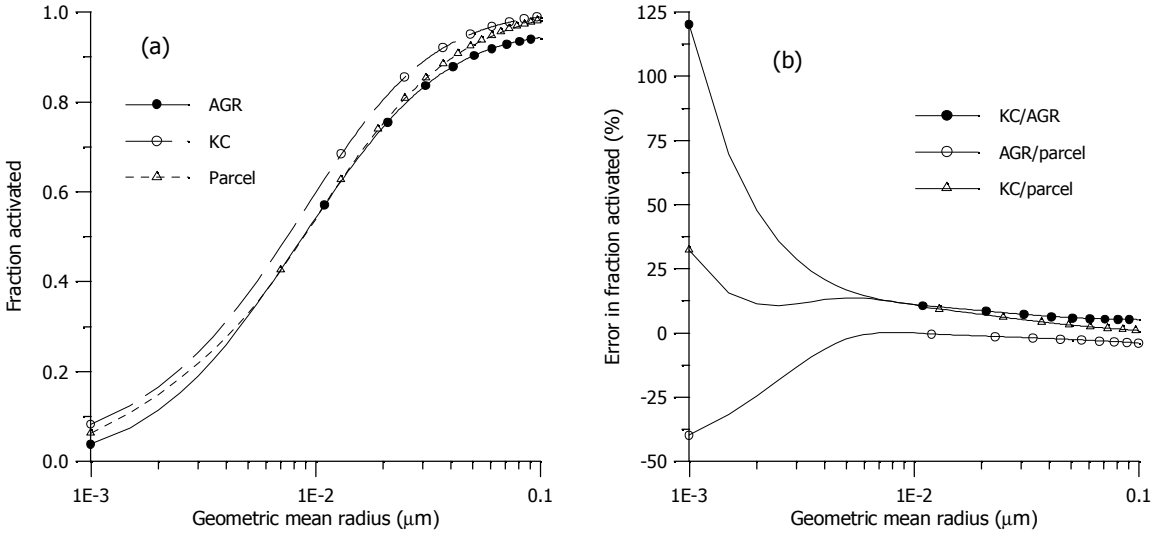

Fig. 2. Comparison of the fraction activated as a function of the mean geometric radius r_{d0} calculated with the modified power law of this work (KC) with parameterization from Abdul-Razzak et al. (1998) (AGC) and with results of detailed parcel simulations from AGC (parcel). (a) fraction activated, N_{dr}/N_a; and (b) relative errors in percent between each two methods as indicated in the legend. Calculations are made at T = 10 ºC, p = 800 mbar, and updraft of 5 m s^{-1}. Aerosol consists of fully soluble ammonium sulfate particles, the size spectrum is lognormal with r_{d0} varied in the range indicated on x-axis, dispersion σ_d = 2.5, total concentration N_a = 200 cm^{-3}. The error between the methods does not exceed 10 % for realistic spectra at $r_{d0} \geq 0.01$ μm and 5 % at $r_{d0} \geq 0.03$ μm.

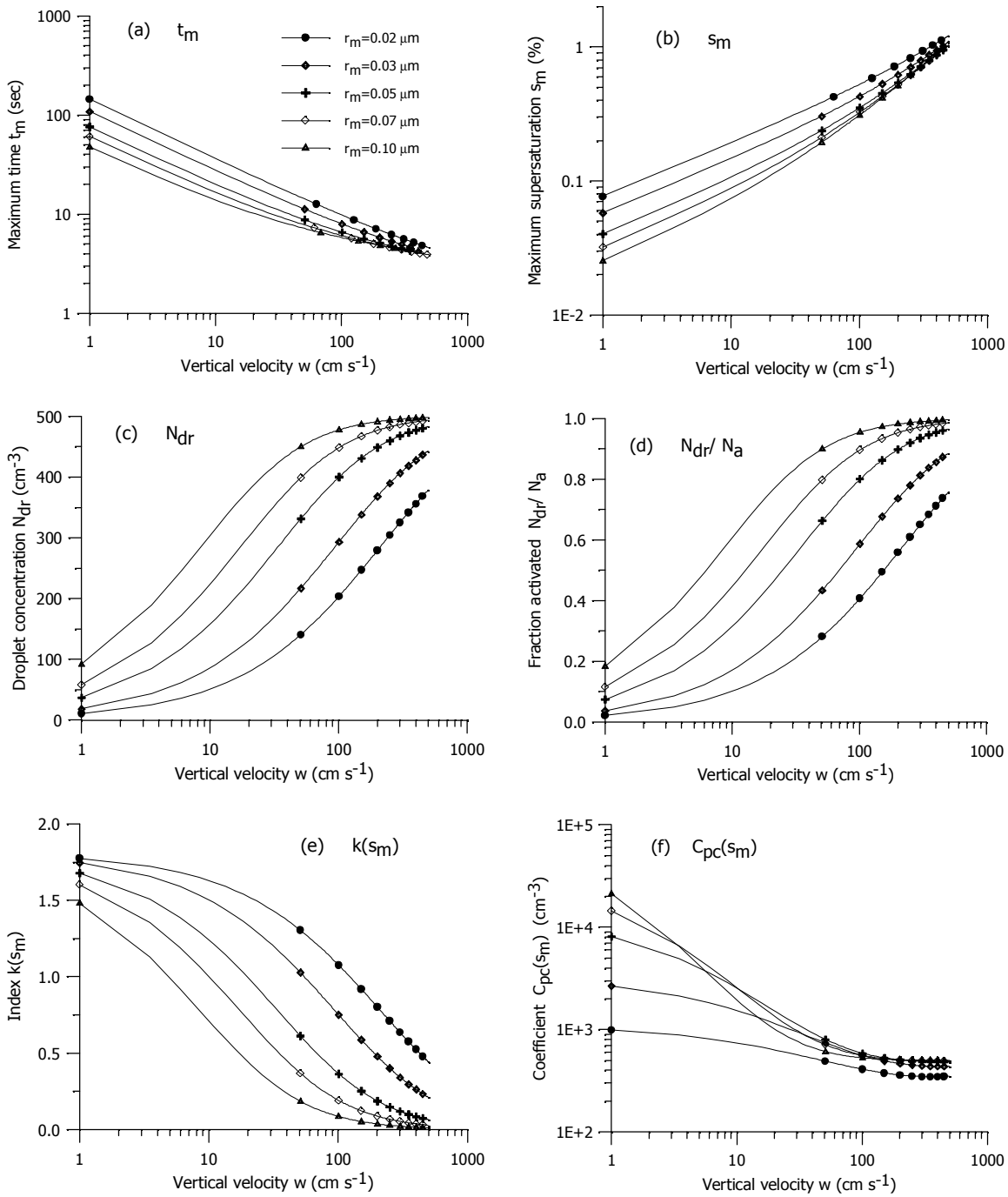

Fig. 3. Effect of variations of the modal radius r_m indicated in the legend. (a) maximum time t_m, sec; (b) supersaturation s_m, %; (c) droplet concentration N_{dr}, cm^{-3}; (d) fraction activated; (e), index $k(s_m)$; (f) coefficient $C_{cp}(s_m)$, cm^{-3} as functions of vertical velocity w calculated with KC06 CCN activity spectrum. Size dispersion $\sigma_d = 1.8$; $\beta = 0.5$ (volume soluble fraction), $b = 0.25$ (50 % of ammonium sulfate), CCN concentration is $N_a = 500$ cm^{-3}.

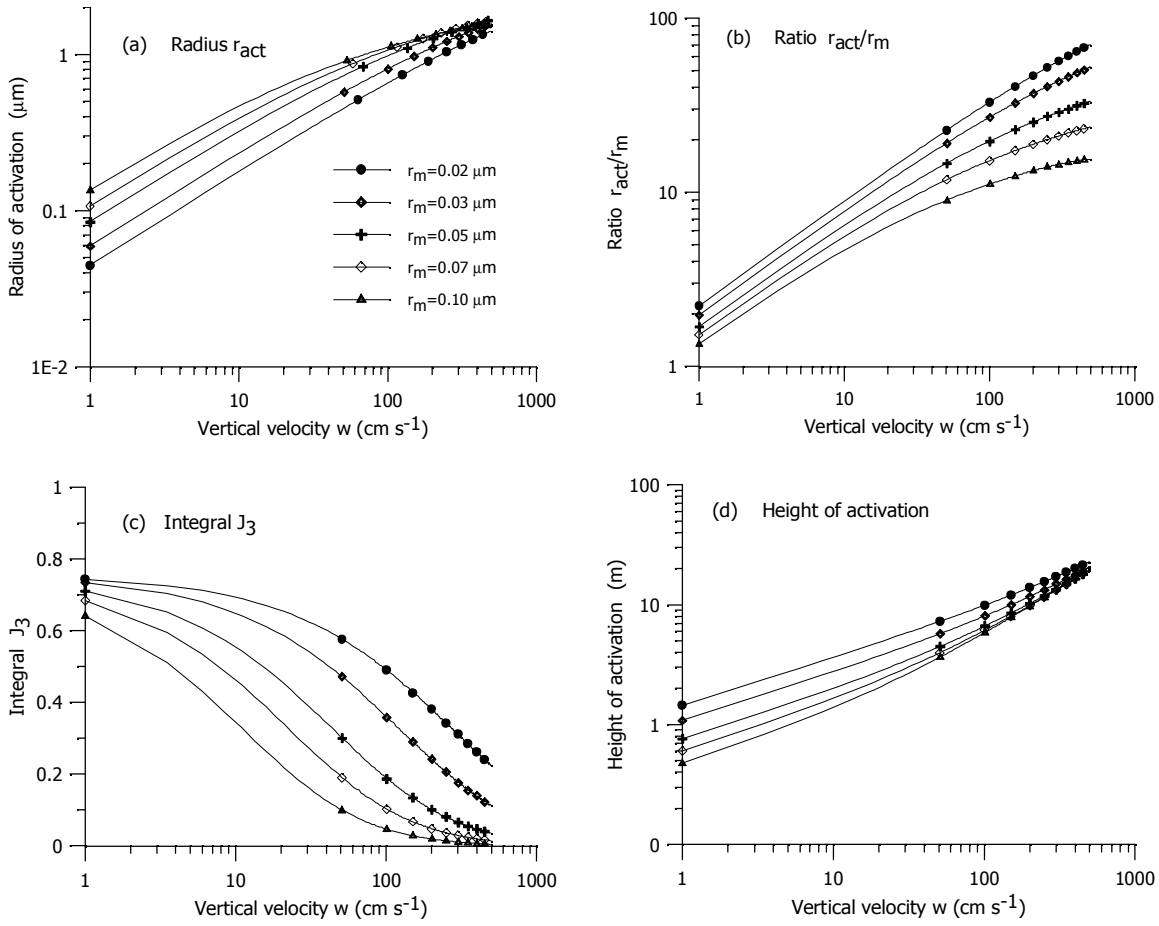

Fig. 4. Additional characteristics of activation. (a) effective radius of activation r_{act} (integral J_0); (b) ratio r_{act}/r_m; (c) Integral J_3; (d) height of activation H_{lift}; input parameters are the same as in Fig. 3.

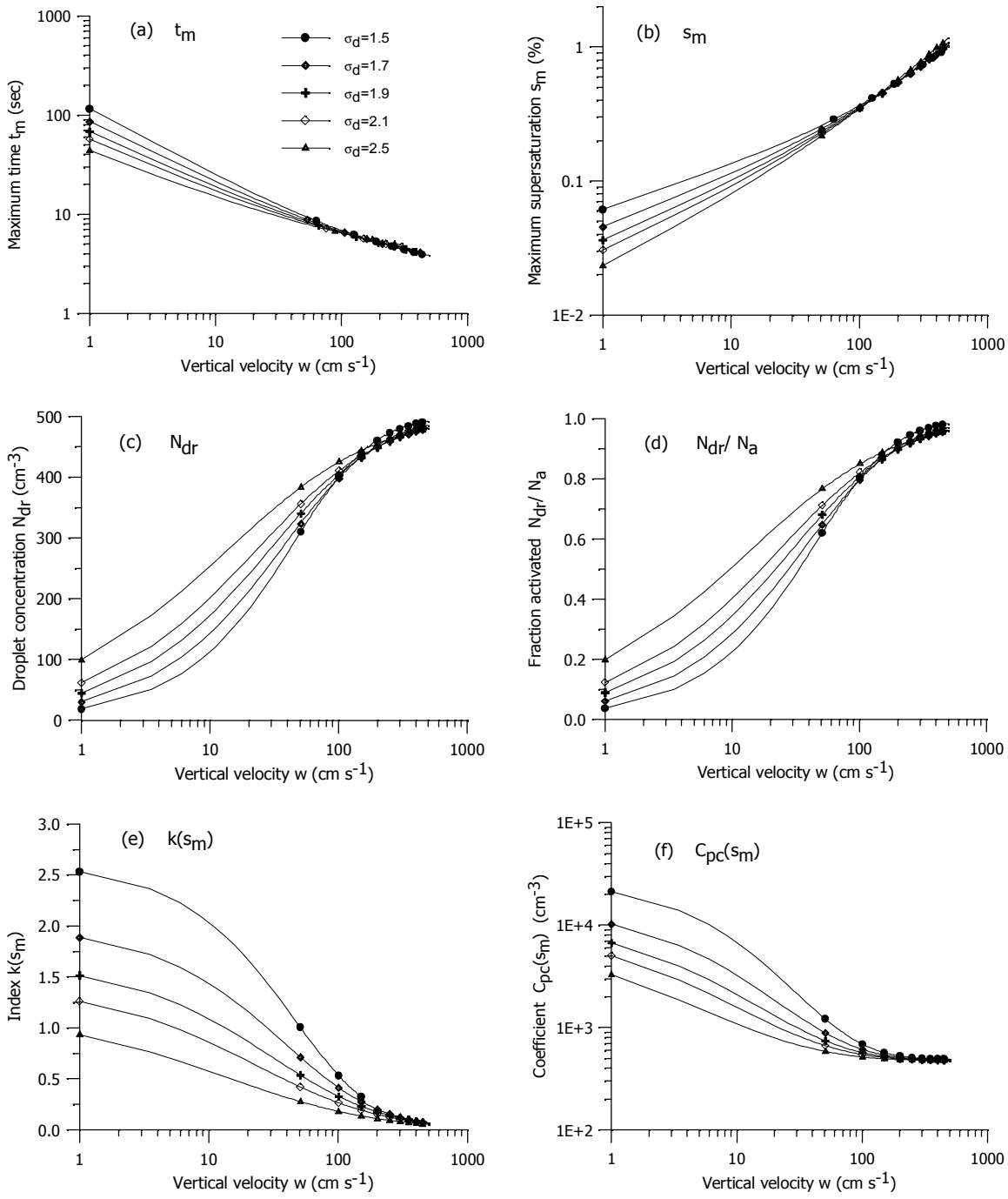

Fig. 5. Effect of variations of size dispersion σ_d indicated in the legend. (a) maximum time t_m, sec; (b) supersaturation s_m, %; (c) droplet concentration N_{dr}, cm^{-3}; (d) fraction activated; (e), index $k(s_m)$; (f) coefficient $C_{cp}(s_m)$, cm^{-3} as functions of vertical velocity w calculated with KC06 CCN activity spectrum. The mean geometric radius r_{d0} = 0.05 μm, β = 0.5 (volume soluble fraction), b = 0.25 (50 % of ammonium sulfate), CCN concentration is N_a = 500 cm^{-3}.

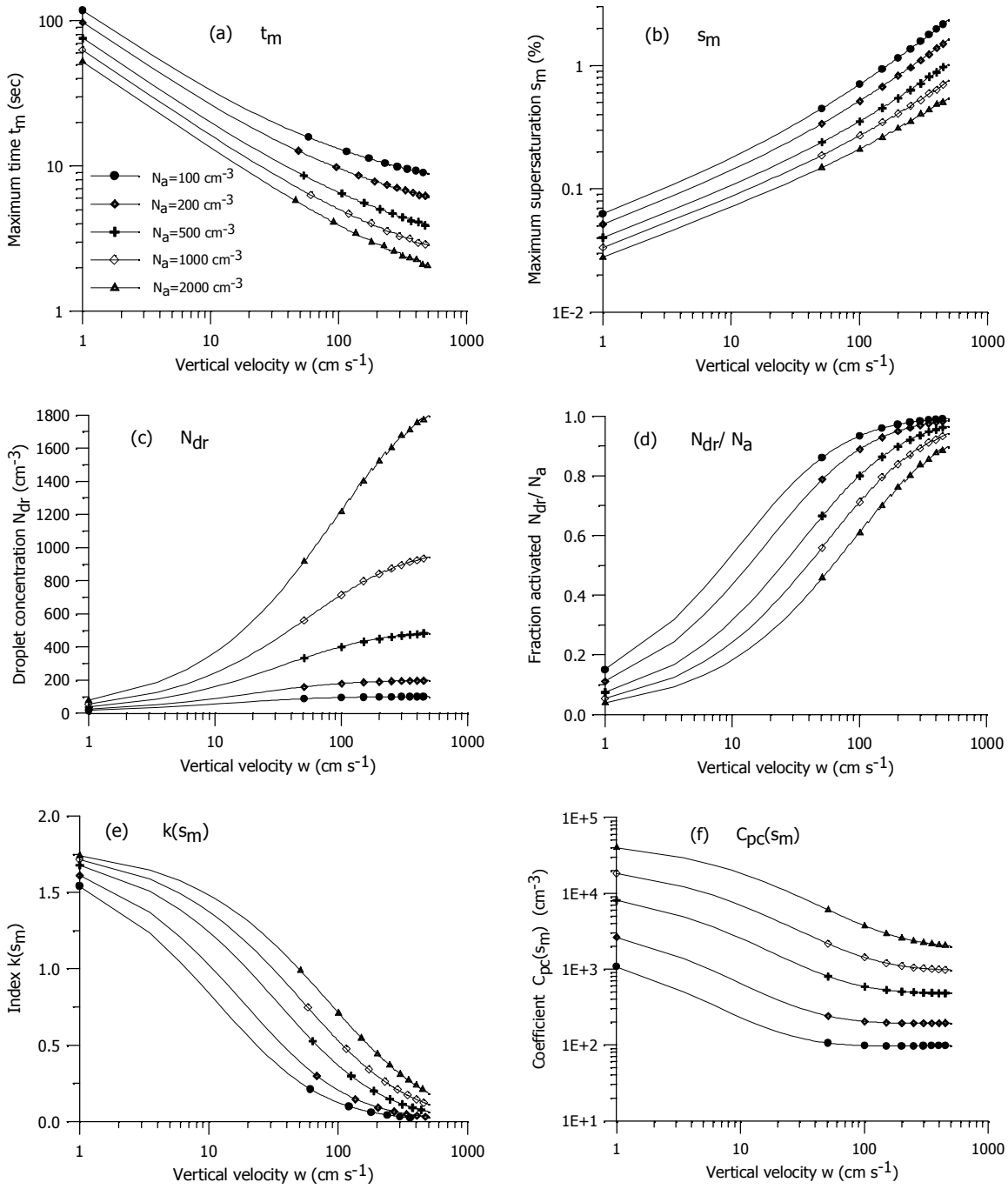

Fig. 6. Effect of variations of CCN concentration N_a indicated in the legend. (a) maximum time t_m, sec; (b) supersaturation s_m, %; (c) droplet concentration N_{dr}, cm^{-3}; (d) fraction activated; (e), index $k(s_m)$; (f) coefficient $C_{cp}(s_m)$, cm^{-3} as functions of vertical velocity w calculated with KC06 CCN activity spectrum. The mean geometric radius r_{d0} = 0.05 μm, σ_d = 1.8, β = 0.5 (volume soluble fraction), b = 0.25 (50 % of ammonium sulfate).

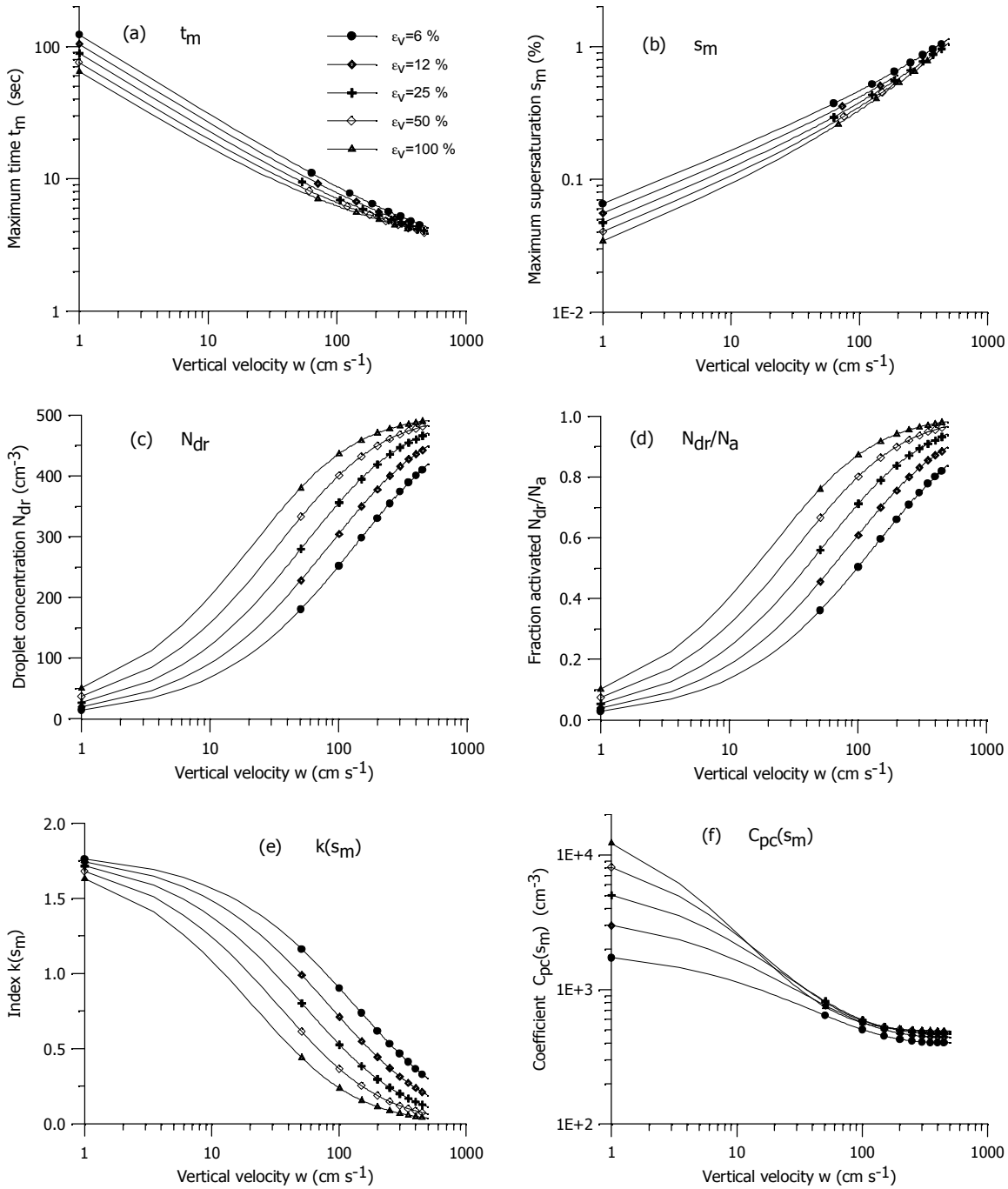

Fig. 7. Effect of variations of soluble fraction ε_v of ammonium sulfate from 6 % to fully soluble nuclei (100 %) indicated in the legend. (a) maximum time t_m, sec; (b) supersaturation s_m, %; (c) droplet concentration N_{dr}, cm^{-3}; (d) fraction activated; (e), index $k(s_m)$; (f) coefficient $C_{cp}(s_m)$, cm^{-3} as functions of vertical velocity w calculated with KC06 CCN activity spectrum. The mean geometric radius r_{d0} = 0.05 μm, σ_d = 1.8, β = 0.5 (volume soluble fraction), N_a = 500 cm^{-3}.

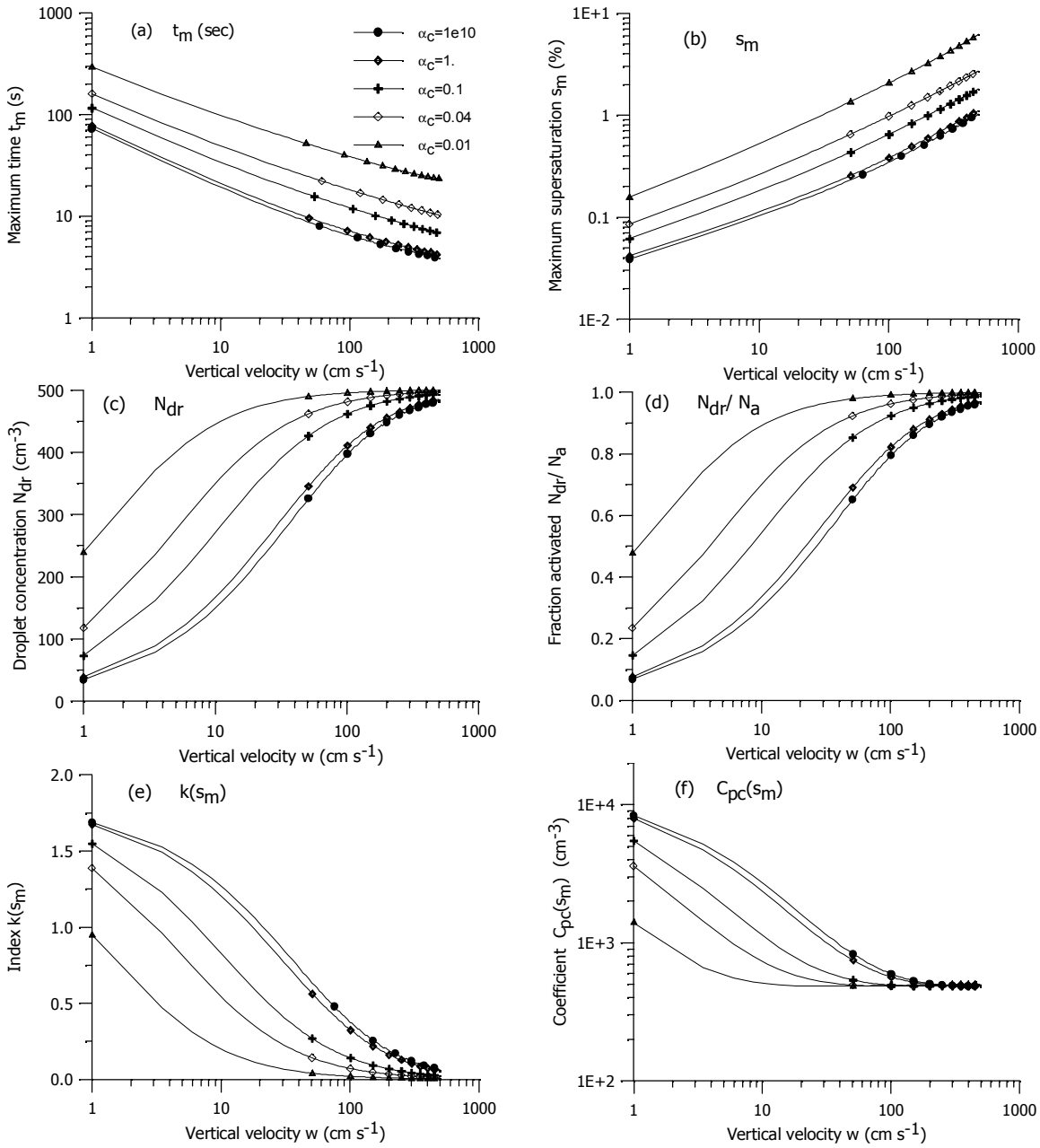

Fig. 8. Effect of variations of condensation coefficient α_c indicated in the legend ($\alpha_c = 10^{10}$ corresponds to $\xi = 0$). (a) maximum time t_m, sec; (b) supersaturation s_m, %; (c) droplet concentration N_{dr}, cm^{-3}; (d) fraction activated; (e), index $k(s_m)$; (f) coefficient $C_{cp}(s_m)$, cm^{-3} as functions of vertical velocity w calculated with KC06 CCN activity spectrum. The mean geometric radius $r_{d0} = 0.05$ μm, $\sigma_d = 1.8$, $\beta = 0.5$ (volume soluble fraction), $b = 0.25$ (50 % of ammonium sulfate), CCN concentration is $N_a = 500$ cm^{-3}.

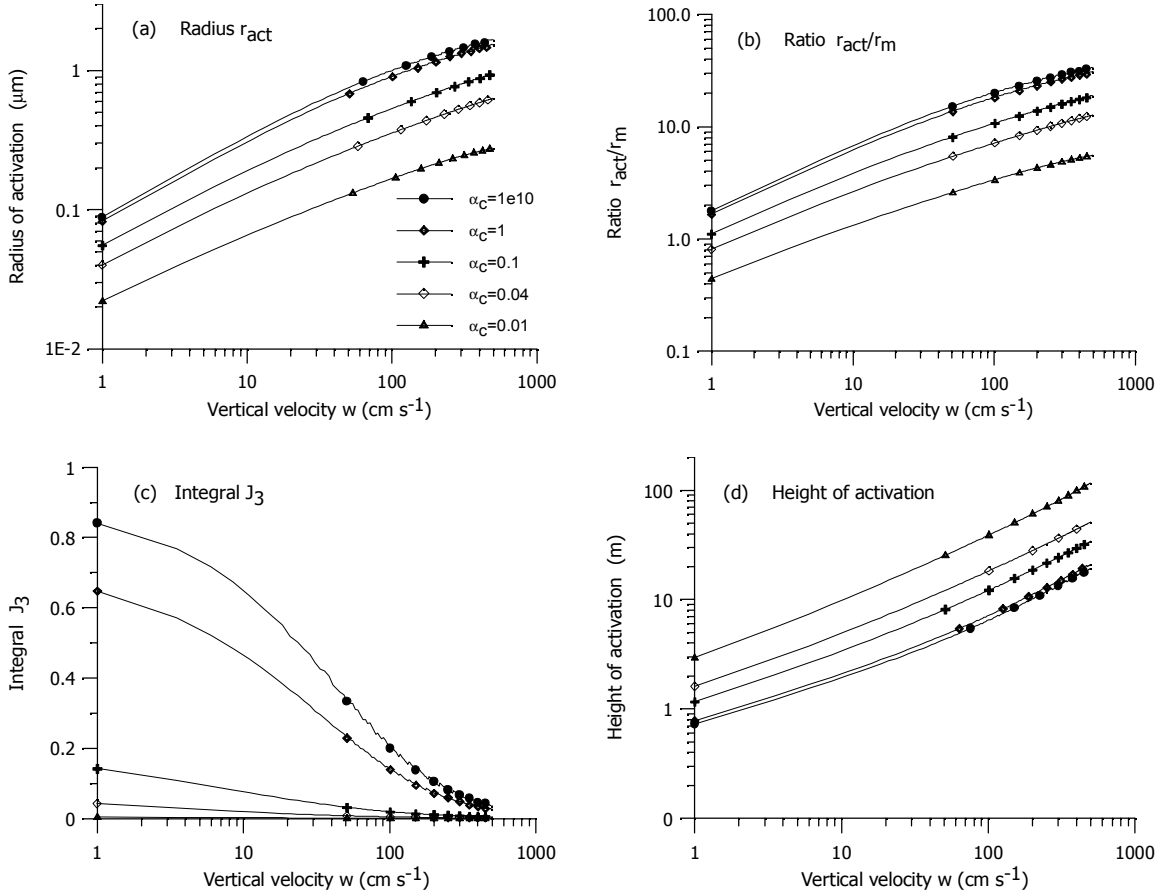

Fig. 9. Effect of variations of condensation coefficient α_c indicated in the legend ($\alpha_c = 10^{10}$ corresponds to $\xi = 0$). (a) effective radius of activation r_{act} (integral J_0); (b) ratio r_{act}/r_m; (c) Integral J_3; (d) height of activation H_{lift}; input parameters are the same as in Fig. 8.

($\alpha_c = 10^{10}$ corresponds to $\xi = 0$).